Lecture 13: AFM imaging of proteins and peptides: *in situ study of the dynamic structural change*

- The goal is to learn the uniqueness and criticalness of *in situ AFM imaging* of **proteins** and **peptides** (or small proteins); (hint: what makes proteins uniquely functional?)
- Case studies:

1. High-resolution imaging of dimeric arrays of rhodopsins;
2. Location and orientation of cytochrome P450 in lipid bilayers;
3. Voltage and pH-induced channel closure of porin OmpF;
4. Imaging of amyloid-β peptides --- critical for Alzheimer disease.

Overview of proteins

- Proteins are crucial for living cells and organisms; the human body contains about 50,000 different kinds of proteins.
- Different proteins are located in different places, plasma, inside-membranes, and inside cells.
- A wide variety of functions of proteins: signal transducing (vision system, smelling system, 2004 Nobel Proze in Medicine), energy transport (respiration system, oxygen delivery), electron transport (photosynthesis, redox reactions), ion channels (membrane structure, 2003 Nobel Proze in Chemsitry), replication of proteins (binding to DNA) …..
- Challenges for structural characterization: NMR (large molecules and interference of lipids and other like), X-ray (difficulties in crystallization, particularly for membrane proteins which require lipid stabilization).
- Advantages of AFM: in situ measurement (in solution), tunable force (minimizing damage or distortion of protein structure), no sample pre-treatment needed, atomic resolution, different imaging modes like LFM, phase, tapping, contact..

Example # 1: AFM imaging of membrane proteins

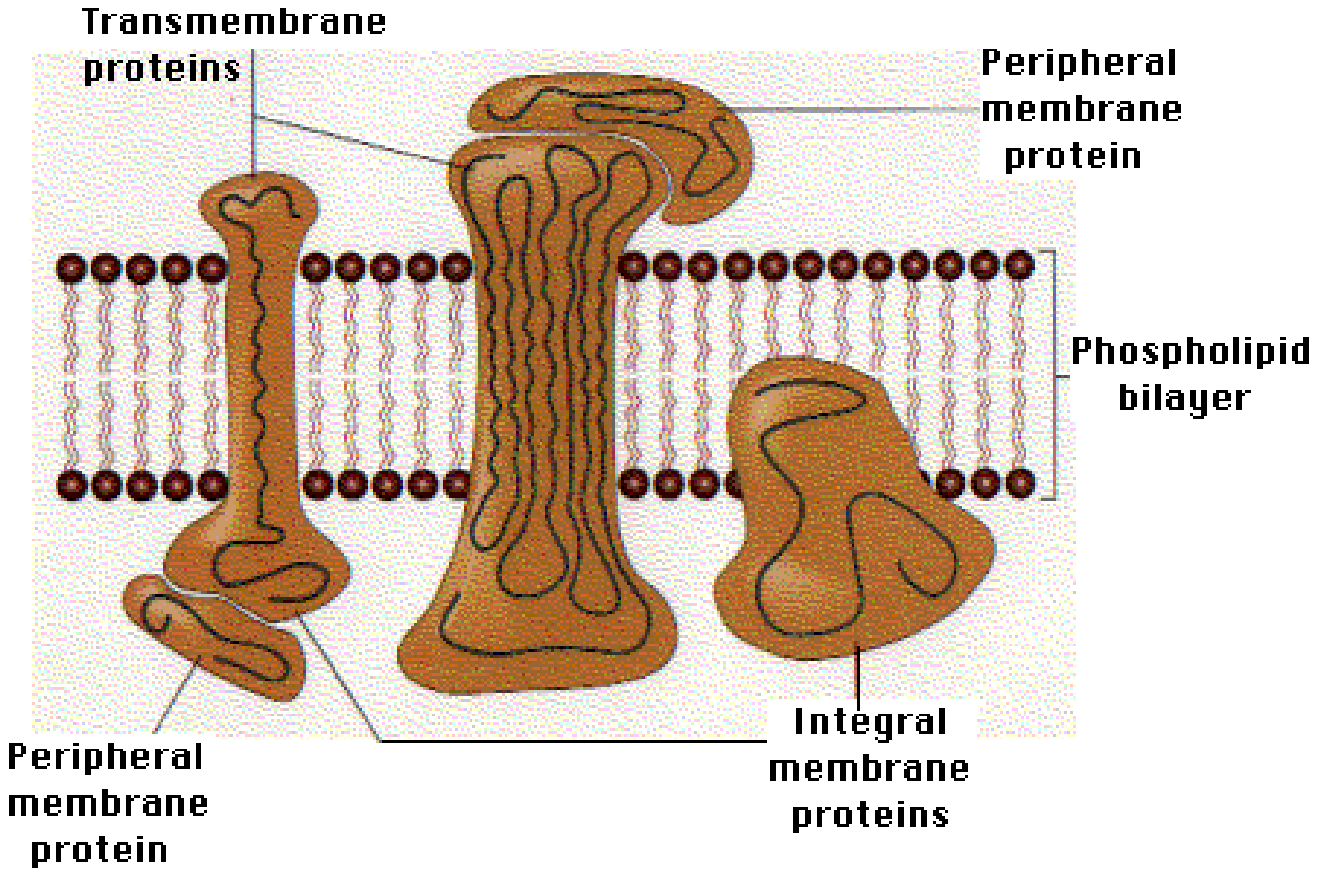

Example # 1: AFM imaging of membrane proteins

- Membrane Proteins are located inside (*trans or not-trans-membrane*) cell membranes (lipid bilayer);
- Membrane Proteins function as **signal transducer** (*smelling, 2004 Nobel in Medicine,* or for light signal transduction as evidenced in the vision systems of mammals) and **ion channels** (***2003 Nobel in Chemistry***).
- One major family of Membrane Proteins is G-protein coupled receptor proteins (**GPCR**). *See slide.*
- *~ 50% of recently launched drugs are targeted against GPCRs with annual sales > $ 30 billion.*
- Probably the most challenging protein in terms of experimental handling: separation, purification, stabilization, and characterization.
- Challenges for X-ray characterization: hard to be crystallized due to the presence of lipids or detergents (stabilizers).
- Challenges for NMR characterization: large molecules and interference of lipids and other like).
- --- *little structural information available prevents reliable modeling and prediction of the protein interactions which are crucial for understanding the biological functions*.
- AFM has been emerging as a unique tool …

The Nobel Prize in **Physiology or Medicine 2004**

"for their discoveries of odorant receptors and the organization of the olfactory system"

Richard Axel

Columbia University
New York, NY, USA; Howard Hughes Medical Institute

Linda B. Buck

Fred Hutchinson Cancer Research Center
Seattle, WA, USA

Heinrich Rohrer and Gerd Binnig

The Nobel Prize in Chemistry 2003

"for structural and mechanistic studies of ion channels"

Peter Agre

Johns Hopkins University School of Medicine
Baltimore, MD, USA

Roderick MacKinnon

Rockefeller University
New York, NY, USA;
Howard Hughes Medical Institute

Rhodopsin Protein: *a typical GPCR*

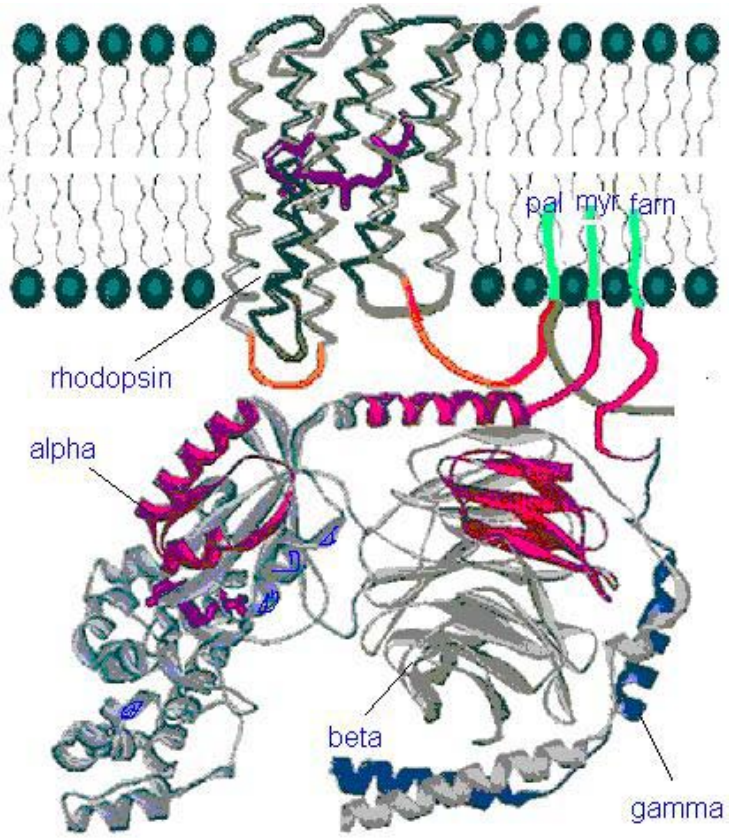

Dimeric arrays of **rhodopsin** proteins

*By **Kris Palczewski** group @ U Washington*

- *Nature* 2003, **421**, 127 - 128;
- *J. Biological Chemistry*, 2003, **278**, p21655.

Another breakthrough: X-ray for Rhodopsin

- *Science*, 2000, **289**, 739-745.

Location of rhodopsin

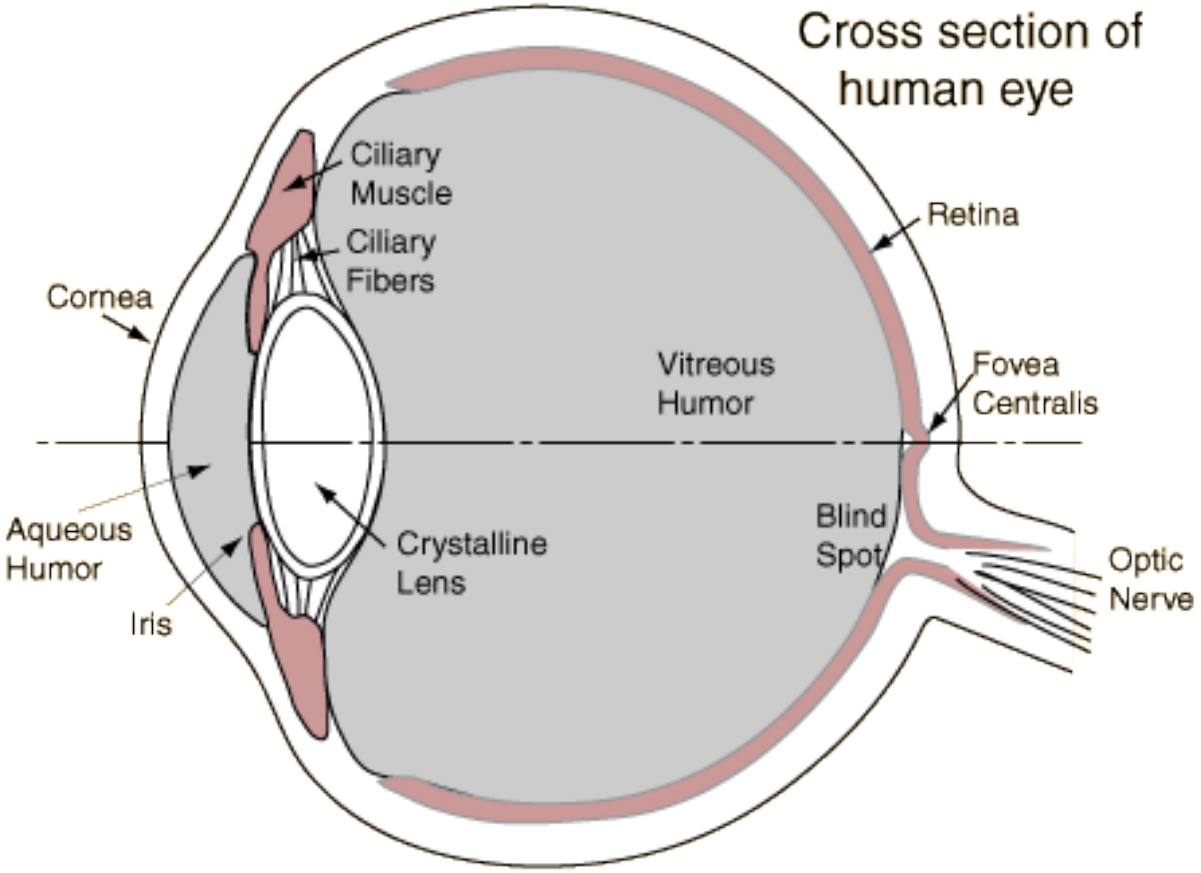

The most sensitive photon-detector ever known.

Camera film: manmade retina for optical recording

The Nobel Prize in Physics 2009

"for the invention of an imaging semiconductor circuit – the CCD sensor"

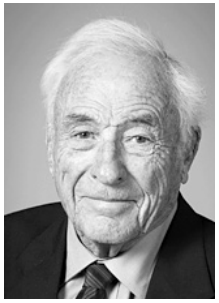

Willard S. Boyle

Johns Hopkins University School of Medicine
Baltimore, MD, USA

George E. Smith

Rockefeller University
New York, NY, USA;
Howard Hughes Medical Institute

A fun: Find your blind spot

close your right eye. With your left eye, look at the red circle. Slowly move your head closer to the image. At a certain distance, the blue line will not look broken!!

Section structure of human outer retina

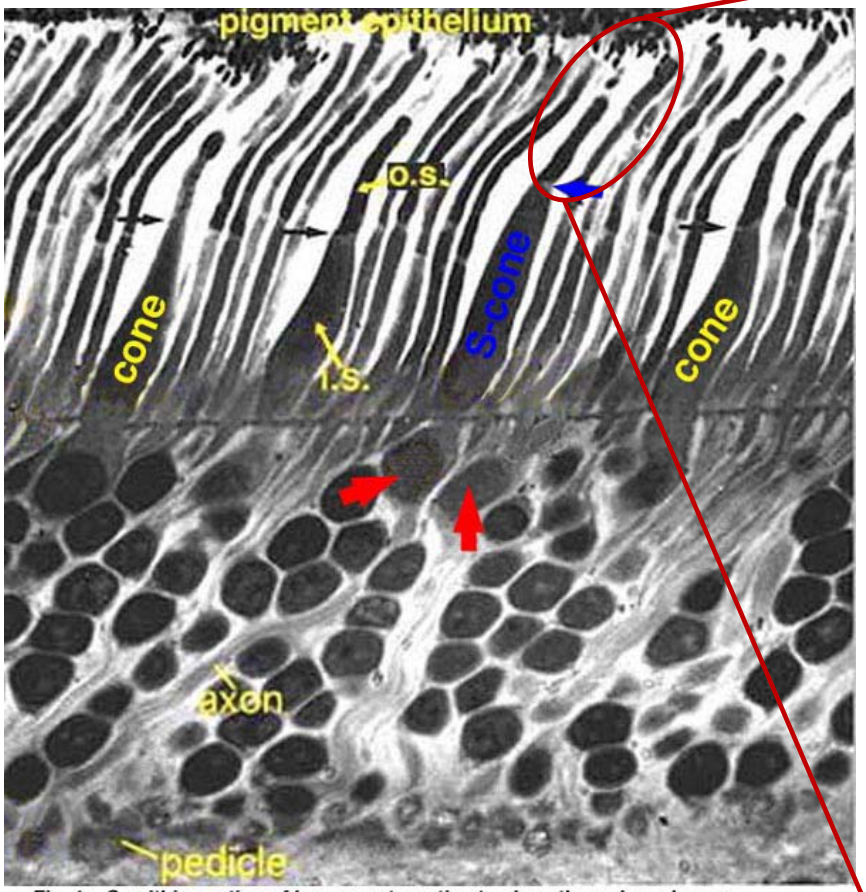

Fig. 1a. Semithin section of human outer retina to show the rods and cones. Short wavelength cones (blue cones) are commonly found occurring next to a neighbouring longer wavelength cone (red arrows).

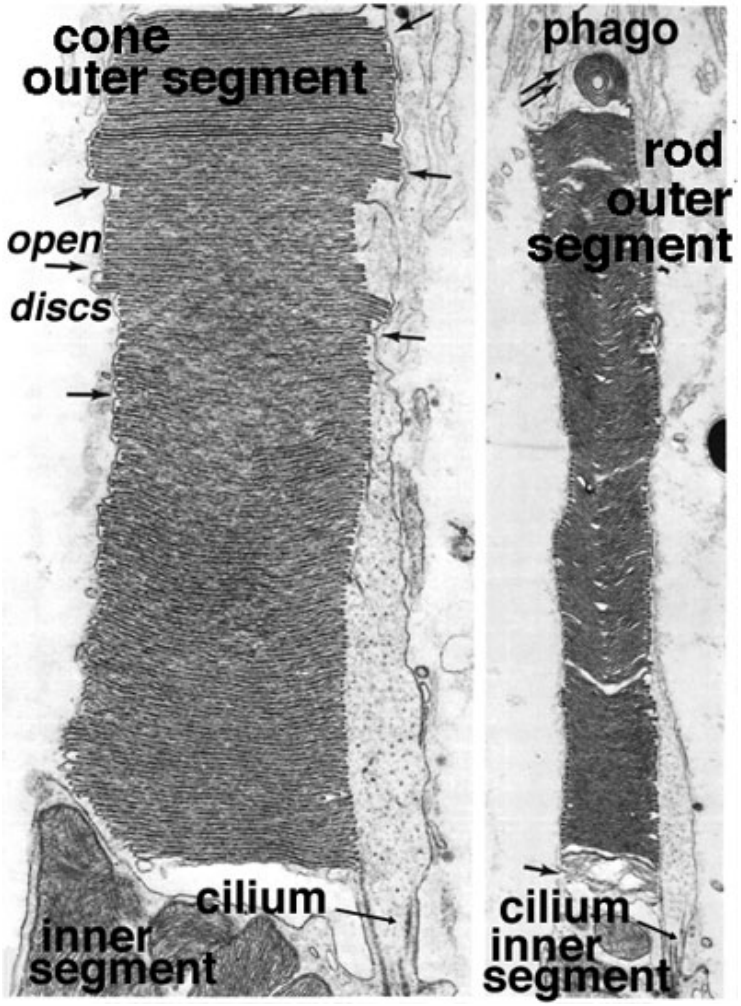

Vertical section of human retina consists of rods and cones nicely aligned, which can be easily distinguished.

Photoreceptor outer segments and the disc structures (From Carlos Rozas, CanalWeb, Chile).

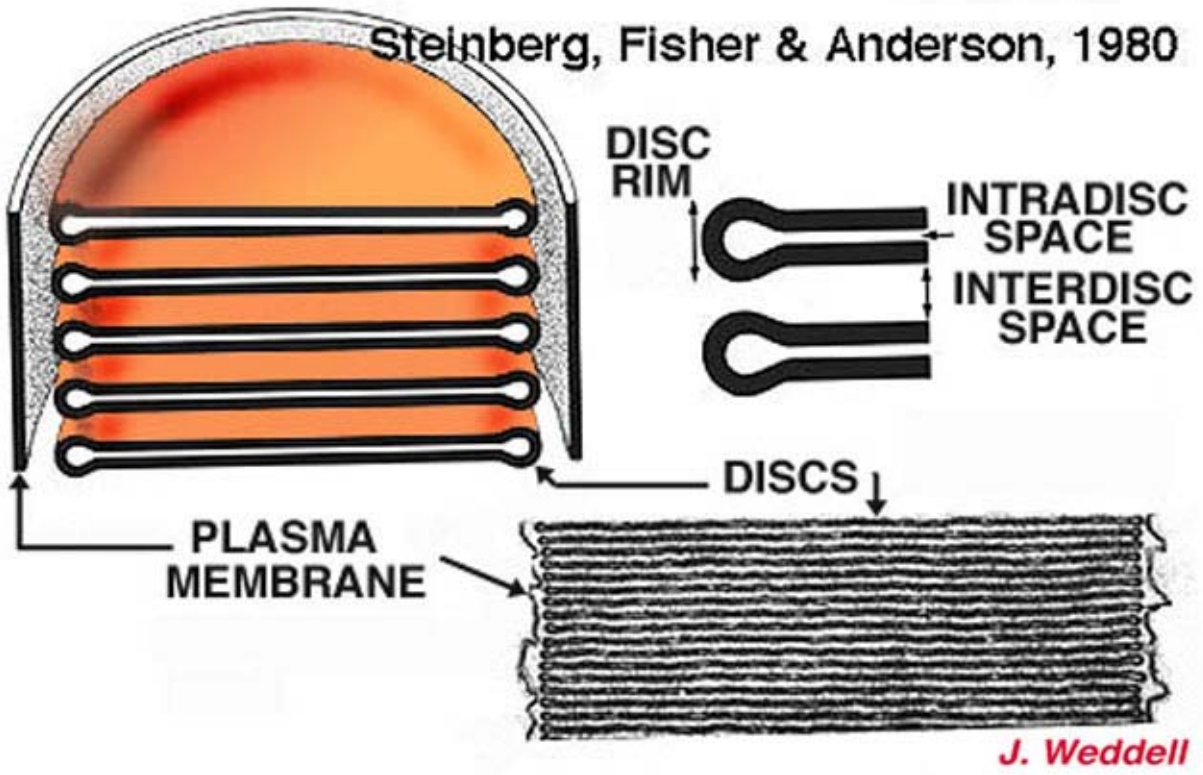

Fig. 6. Drawing of rod outer segment discs.

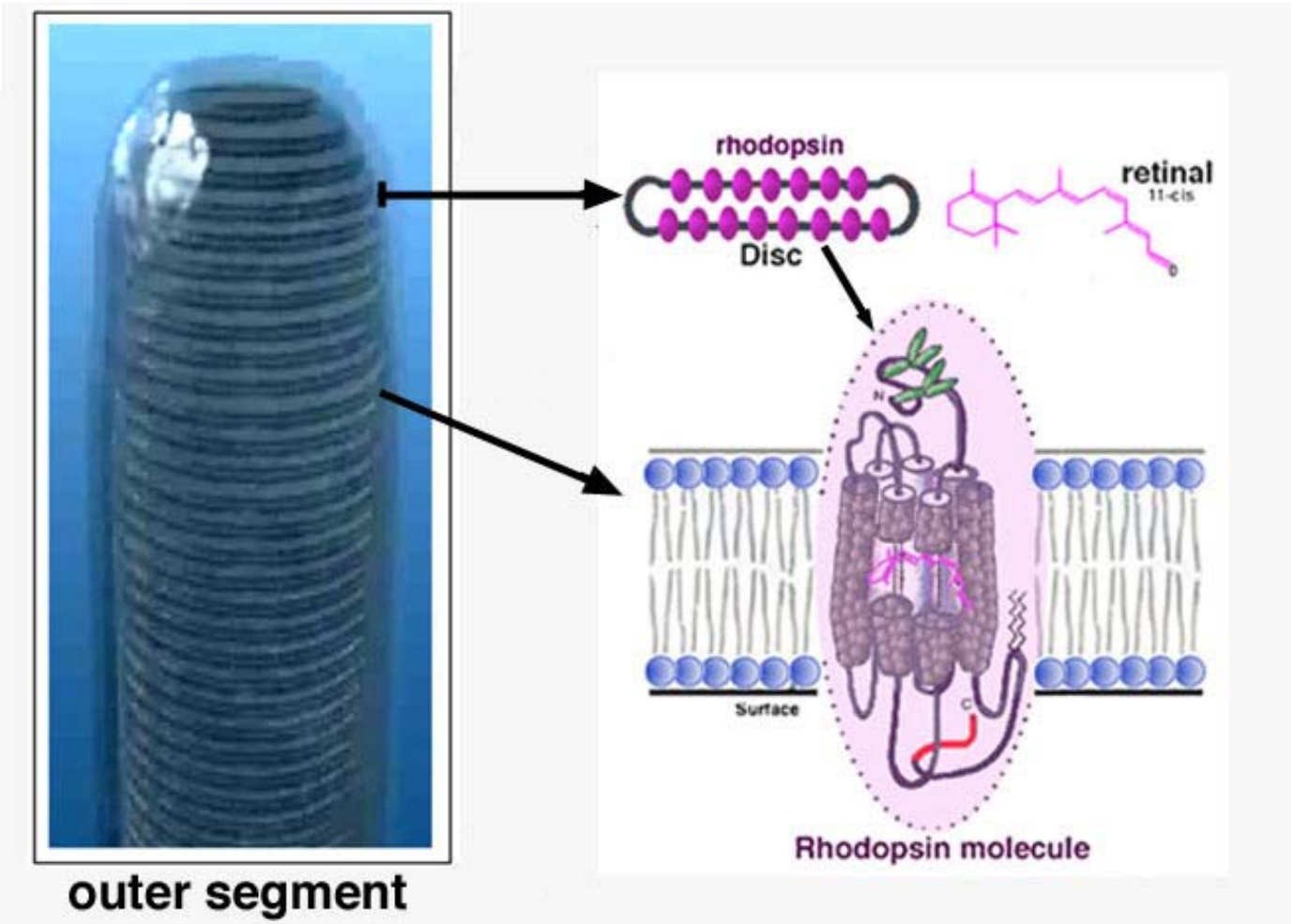

Fig 8. Schematic diagram of Rhodopsin in the outer segment discs.

Rhodopsin: *the first and one of the only few GPCR proteins that gets X-ray crystalline structure.*

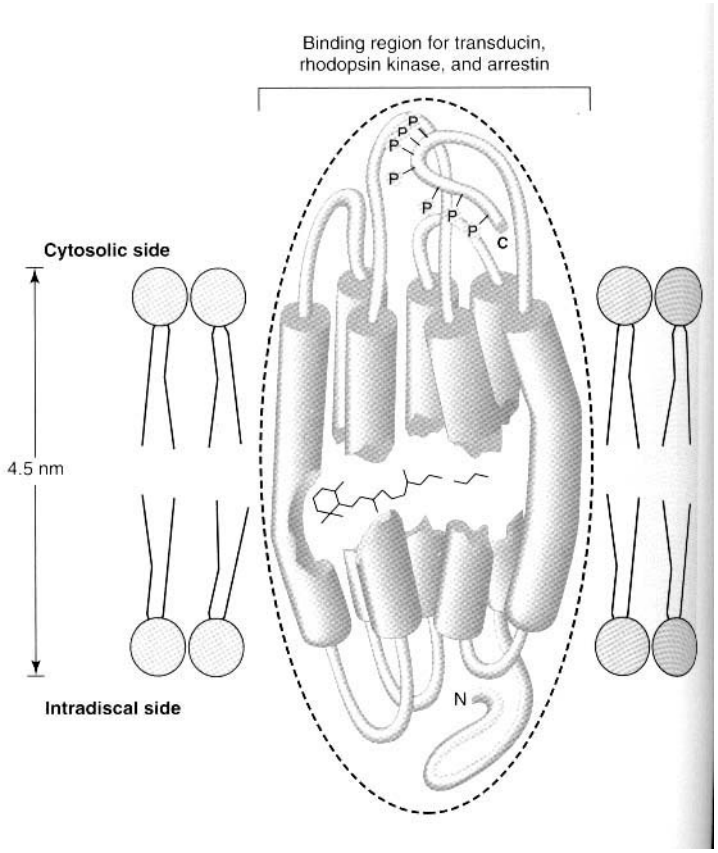

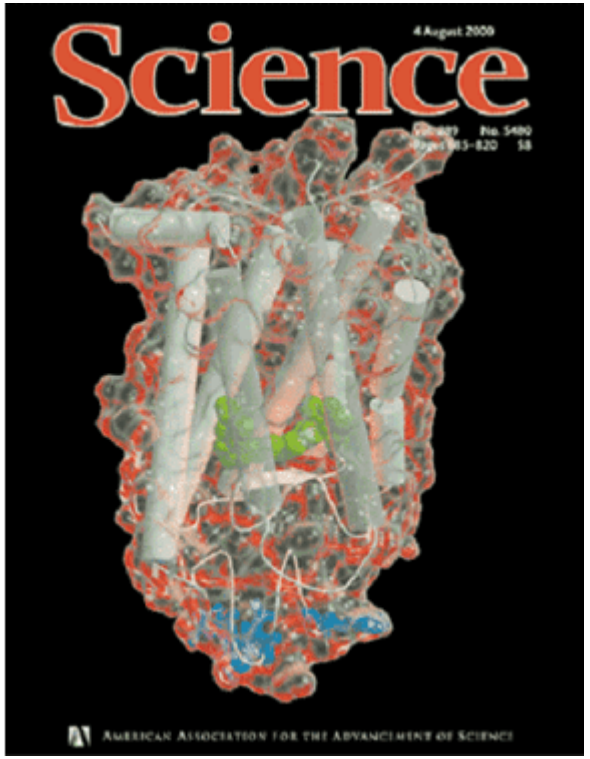

Kris Palczewski *Science*, 2000, **289**, 739-745

But, how rhodopsin proteins are packed and organized to afford the optimized sensitivity?

Large surface exposure:

that's how sensitive and smart the vision system acts

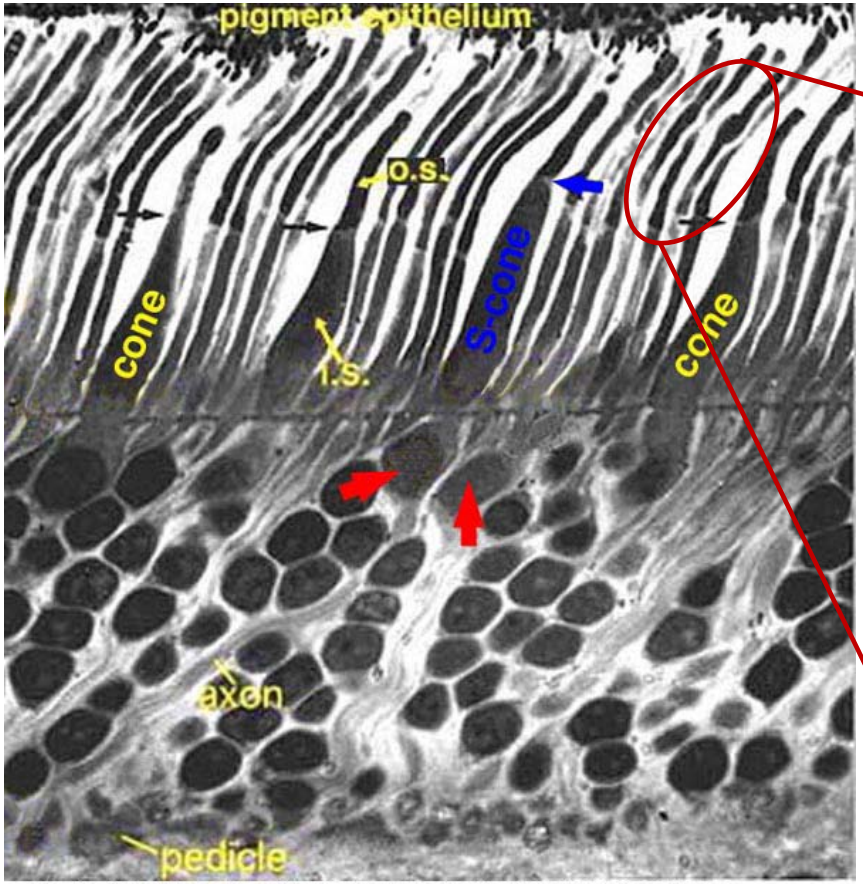

Fig. 1a. Semithin section of human outer retina to show the rods and cones. Short wavelength cones (blue cones) are commonly found occurring next to a neighbouring longer wavelength cone (red arrows).

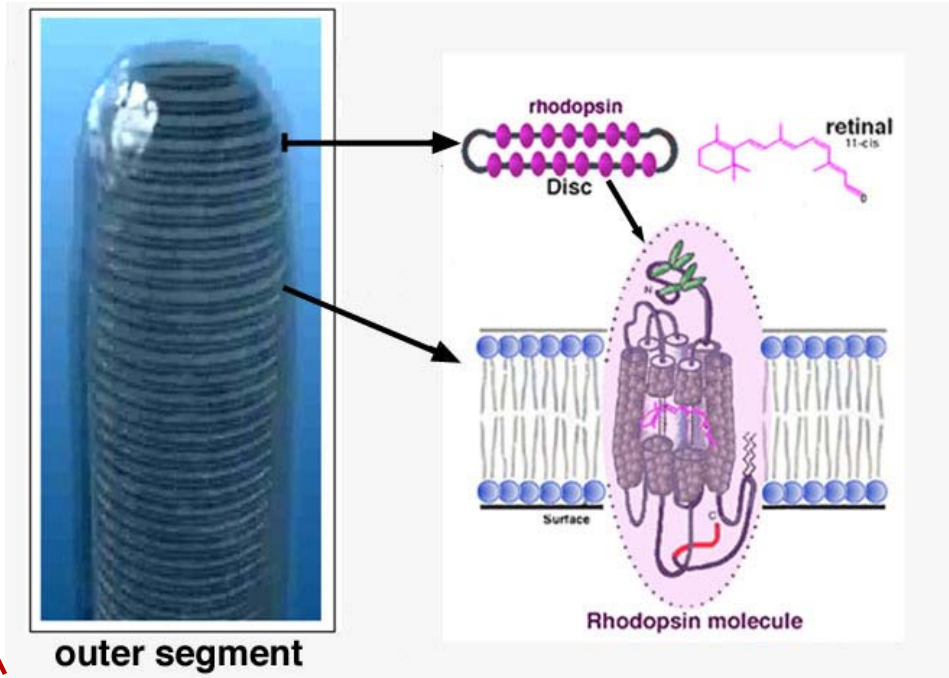

Fig 8. Schematic diagram of Rhodopsin in the outer segment discs.

Isolation and characterization of mouse ROS

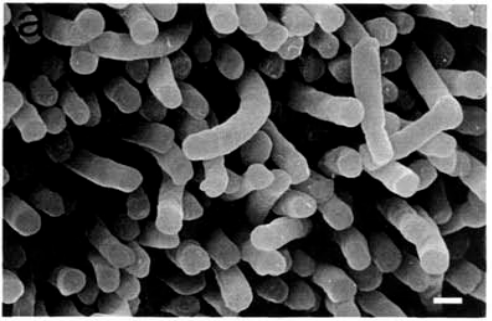

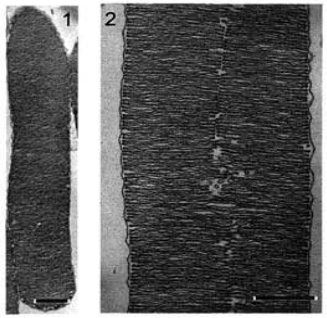

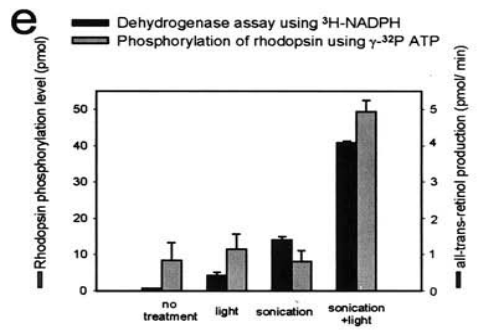

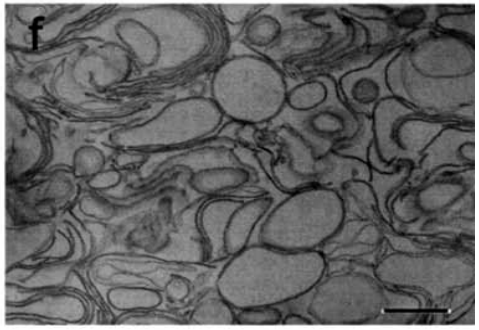

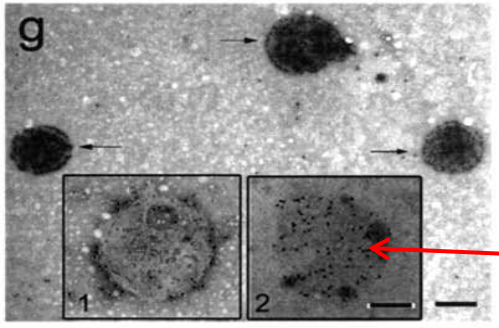

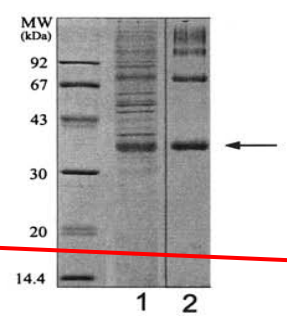

a, SEM of **mouse rod outer-segment (ROS)** attached to the retina.

b, light micrograph of isolated ROS indicating the purity of the preparation.

c, SEM of isolated ROS.

d, TEM of lower and higher magnifications of isolated sectioned ROS. Disks are arranged in a stack and are surrounded by the plasma membrane (*panel 1*). An incisure running through the ROS can be discerned at a higher magnification (*panel 2*). Each disk has cytoplasmic and extracellular (intradiscal) surfaces and a rim region that joins the two layers of the bilayer.

e, permeability of ROS as tested using phosphorylation of rhodopsin and redox reactions. The *gray bars* show the assays of rhodopsin phosphorylation of intact ROS under different conditions. The *black bars* represent the dehydrogenase assays using [C4-3H]NADPH under different conditions.

f, EM of isolated disks prepared by thin sectioning. Isolated disks appeared as **vesicles**.

g, EM of immuno**gold**-labeled and negatively stained isolated disks. The *arrows* indicate native disks exposing the cytoplasmic surface, which is labeled with the 1D4 antibody specific toward the C terminus of rhodopsin.

Inset 1, membrane from burst disk exposing the extracellular surface and incubated with antibody 1D4. Gold particles are observed at the periphery of the disk.

Inset 2, same as *inset 1* but incubated with antibody 4D2 against the N terminus of rhodopsin. Gold particles are evenly distributed on the extracellular surface of the disk.

h, Coomassie Blue-stained SDS-polyacrylamide gel of isolated ROS (*lane 1*) and isolated disks (*lane 2*). Rhodopsin is found predominantly as a monomer (*arrow*) but also as a multimer (*lane 2*).

Scale bars: 1 µm (*a*), 6 µm (*b*), 1 µm (*c*), 0.5 µm (*d, 1*), 0.3 µm (*d, 2*), 0.6 µm (*f* and *g*), and 0.3 µm (*insets* in *g*).

Just like a pizza, not much details.

Direct coating with Au

Antibody → N-terminal → Au

Palczewski,JBC,2003,278,21655

ZnO nanorods: sharing the same morphology as image a) above

for applications in optics and photonics like lasers

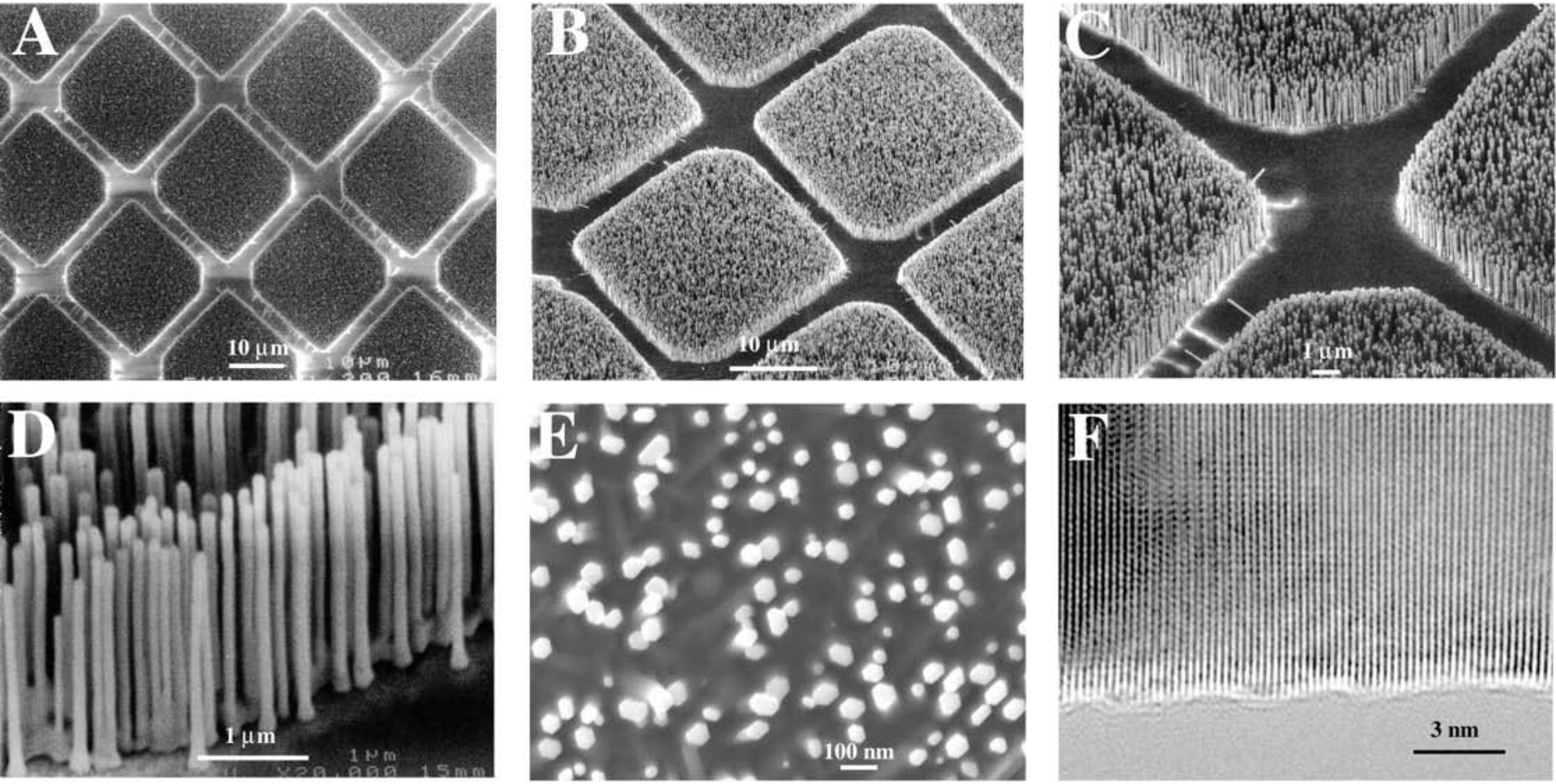

Peidong Yang et al., Science 2001, vol 292, p1987

Some experimental techniques

- Single disks were obtained by osmotic bursting of rod outer-segments.
- Membrane samples were never exposed to light.
- AFM feedback (light lever) uses infra-red instead of red laser
- AFM was carried out on mica, in buffer solution (20 mM Tris–HCl (pH 7.8), 150 mM KCl and 25 mM MgCl2) --- which is typical for stabizing membrane proteins, particularly GPCR.

Challenges for Electronic Microscopy to image the arrangement of proteins within the disc

- Stain or coating distorts the nanostructure of rhodopsins;
- High magnification turns to be hard.

AFM fills the technical gap !

AFM imaging of the disc

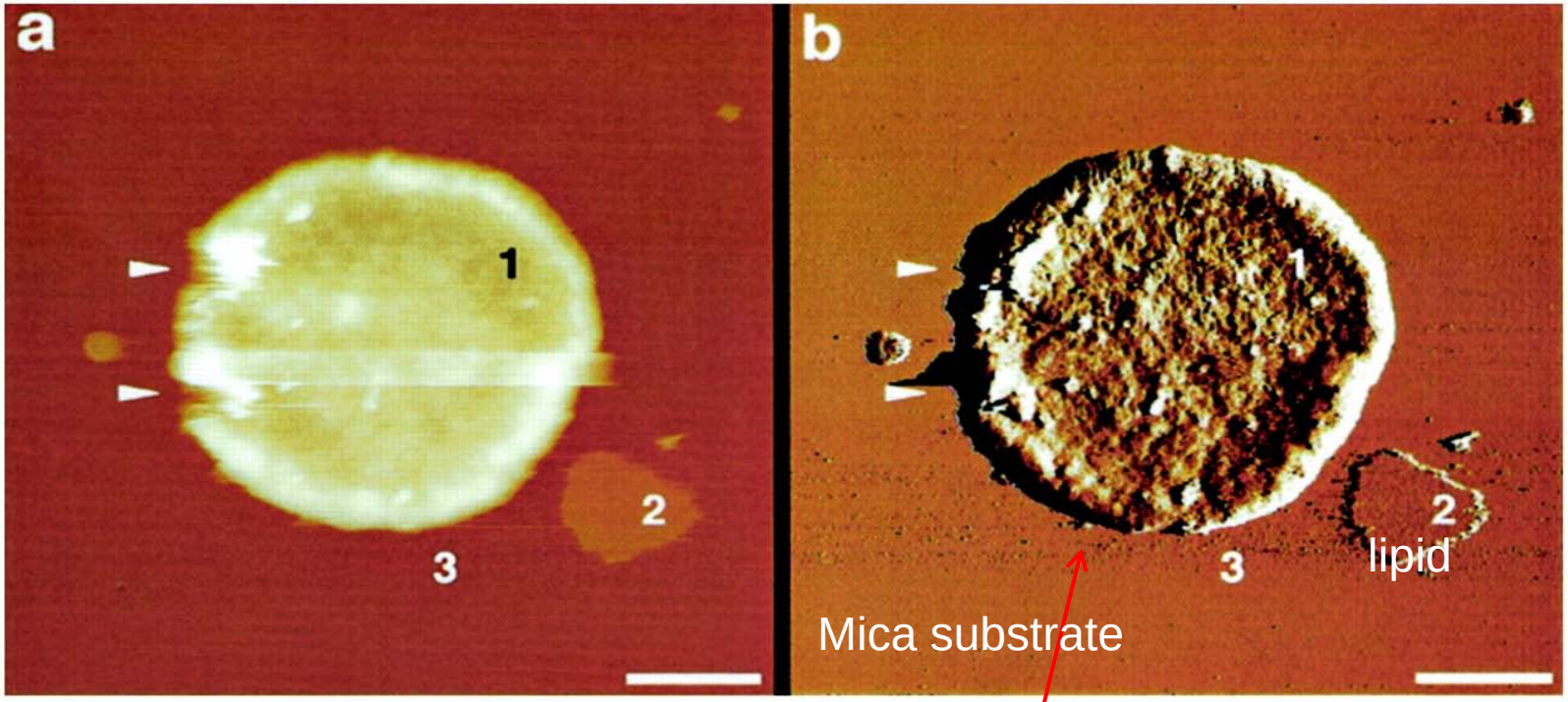

AFM height (*a*) and deflection (*b*) images of an intact disk membrane having a typical thickness of 16–17 nm. Three different surface types are evident: the cytoplasmic surface of the disk (type *1*), co-isolated lipid (type *2*), and mica (type *3*). The deflection image (*b*) reveals that surface type 1 is rough compared with bare lipid (type *2*), indicating the presence of densely packed proteins.

Scale bars: 250 nm (*a* and *b*). Vertical brightness ranges: 60 nm (*a*) and **0.6 nm (*b*).**

Lateral force imaging.

Palczewski,JBC,2003,278,21655

AFM imaging of the disc

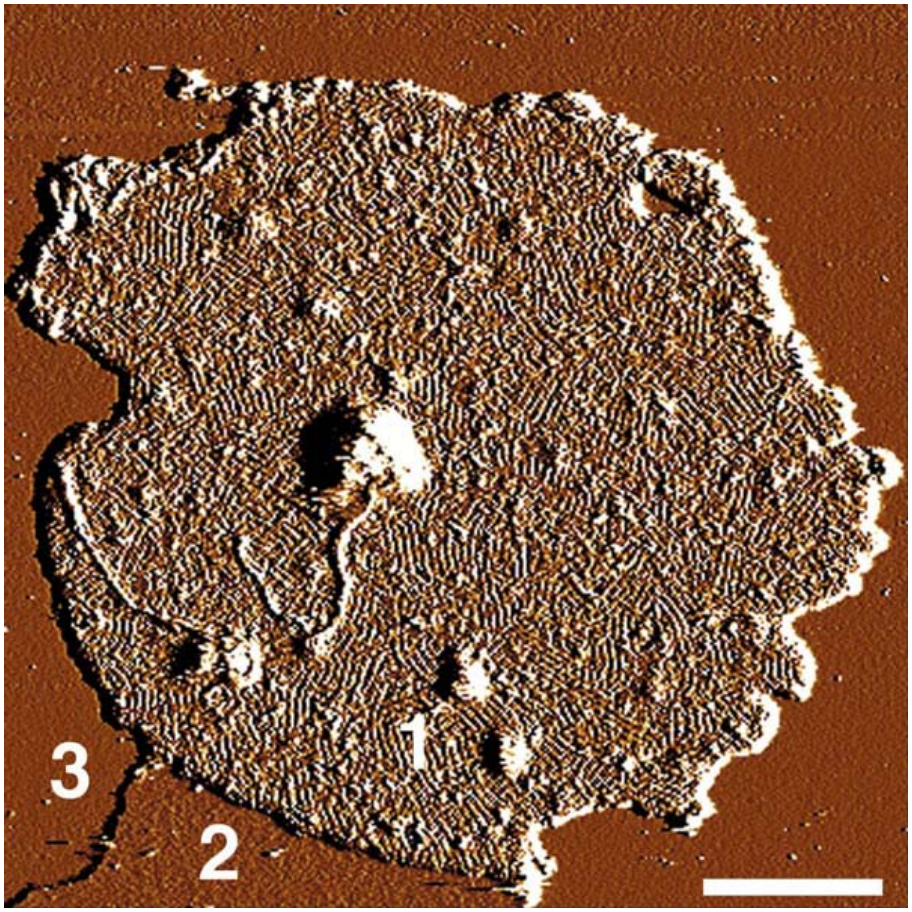

Deflection image of a mouse eye-disc membrane adsorbed on mica, visualized by atomic-force microscopy.
Three different surface types are evident: 1, the cytoplasmic side of the disc membrane; 2, lipid; and 3, mica.
Scale bar, 200 nm.

Organization and topography of the cytoplasmic surface of rhodopsin.

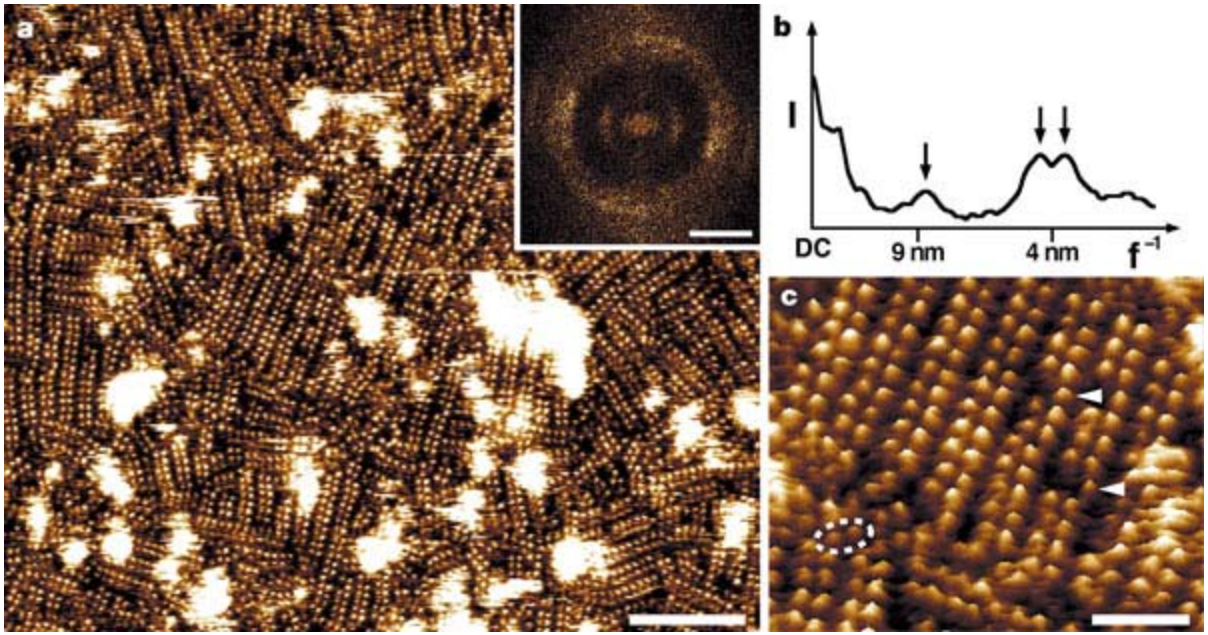

a, AFM Topograph showing the paracrystalline arrangement of rhodopsin dimers in the native disc membrane. Inset, arcs in the calculated powder-diffraction pattern reflect the regular arrangement of rhodopsin in the membrane.
b, Angularly averaged powder-diffraction pattern, showing peaks at $(8.4\ nm)^{-1}$, $(4.2\ nm)^{-1}$ and $(3.8\ nm)^{-1}$.
c, Magnification of a region of the topograph in **a**, showing rows of rhodopsin dimers, as well as individual dimers (inside dashed ellipse), presumably broken away from one of the rows, and occasional rhodopsin monomers (arrowheads). The rhodopsin molecules protrude from the lipid bilayer by 1.4+/- 0.2 nm (*n* = 111). Scale bars: a, 50 nm; inset, (5 nm)-1; **c**, 15 nm.

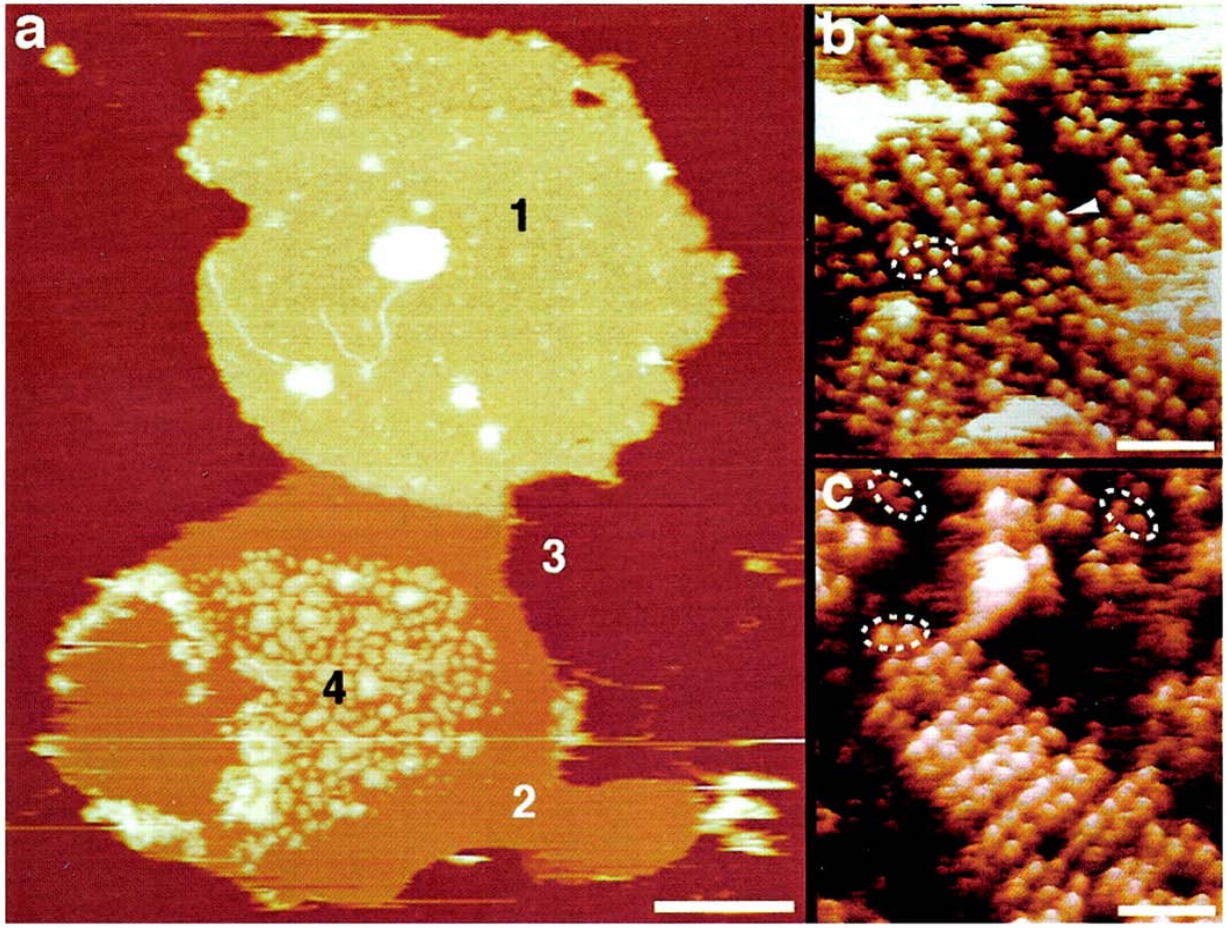

Area 1
More intact

Area 4
More damage

a, Height image of the open, spread-flattened disk. Four different surface types are evident: the cytoplasmic surface of the disk (types *1* and *4*), lipid (type *2*), and mica (type *3*). The topographies of regions 1 (*b*) and 4 (*c*) at higher magnification reveal densely packed rows of rhodopsin dimers.

Scale bars: 250 nm (*a*) and 15 nm (*b* and *c*). Vertical brightness ranges: 22 nm (*a*) and 2.0 nm (*b* and *c*).

Palczewski,JBC,2003,278,21655

Extremely high density → sensitivity

- Average density of rhodopsin monomer: 48,000 μm^{-2}.
- This gives a density of about 3.0×10^{13} In^{-2}.

- The best CCD available for digital camera --- density of photodiode: 40 M/In^2 = 4.0×10^7 In^{-2}

*1,000,000 times lower than the **retina** of even a mouse !!*

Fact:
The eyesight of the Mouse, however, isn't so good and they depend upon their whiskers to guide them, especially in the darkness where their eyes are practically useless.

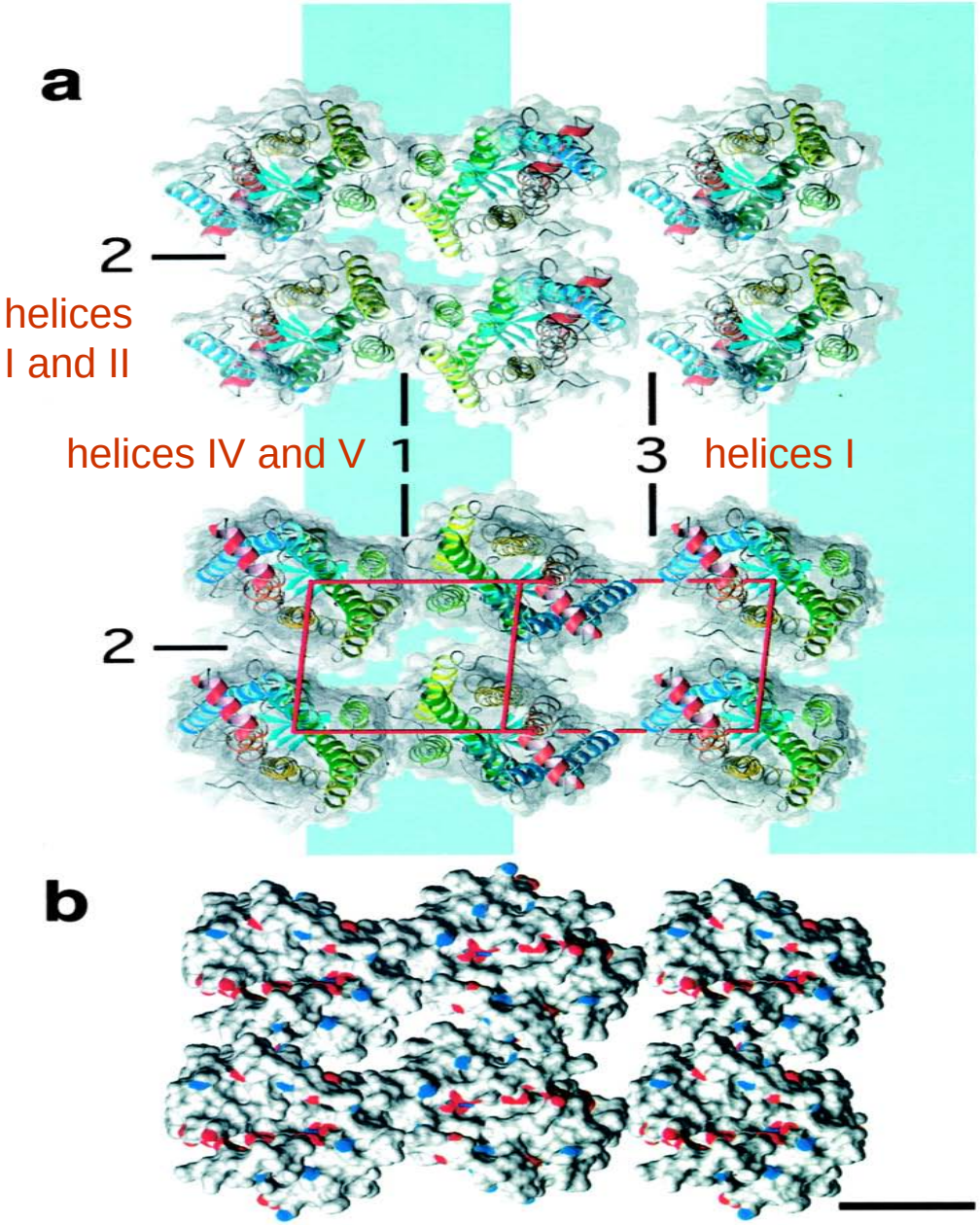

Model for the packing arrangement of rhodopsin molecules within the paracrystalline arrays in native disk membranes.

***a*, rhodopsin assembles into dimers through a contact provided by helices IV and V (contact *1*). Dimers form rows (*highlighted* by a *blue band*) as a result of contacts between the cytoplasmic loop connecting helices V and VI and helices I and II from the adjacent dimer (contact *2*). Rows assemble into paracrystals through extracellular contacts formed by helix I (contact *3*). Only half of the second row is shown. Views: extracellular (*top panel*) and cytoplasmic (*bottom panel*) sides of rhodopsin. Helices of rhodopsin are colored as shown: helix I in *blue*, helix II in *light blue*, helix III in *green*, helix IV in *light green*, helix V in *yellow*, helix VI in *orange*, and helix VII and cytoplasmic helix 8 in *red. b*, surface of rhodopsin molecules showing the locations of charged Glu and Asp (*red*) and Arg and Lys (*blue*) residues. A single line of negative charges is located close to the long groove on the cytoplasmic surface of the rhodopsin dimer. *Scale bar* = 2.5 nm.**

Palczewski,JBC,2003,278,21655

Example # 2: AFM imaging of microsomal cytochrome P450 in nanometer-scale phospholipid bilayer disks

Timothy H. Bayburt*, and Stephen G. Sligar*

Beckman Institute for Advanced Science and Technology, Departments of Biochemistry and Chemistry, University of Illinois, Urbana, IL 61801

Sligar, ***PNAS***, 2002, 99, 6725-6730

cytochromes

- Cytochromes P450 are a class of heme-thiolate enzymes that activate molecular oxygen used in the oxidation of a variety of substrates.
- Multiple functions of P450s --- synthesizing steroids, activating procarcinogens, and metabolizing pharmaceuticals.
- The biological importance leads to a large amount of effort to understand their structure and function.
- Unfortunately, the enzymes are membrane proteins and have proven difficult to characterize through NMR or X-ray, due to the presence of lipids.
- On the other hand, the lipids are crucial for maintaining and modulating the specific function of the enzyme --- *efficient electron transfer from NADPH-cytochrome P450 reductase (P450 reductase) to the P450 heme*.
- The rate of electron transfer has been shown to correlate with the type of lipids in the membrane, the mechanism by which the lipids mediate electron transfer is unclear.
- Probing the lipid-protein structure and interaction is thus highly demanded …

Sligar,PNAS,2002,99,6725-6730

Cytochrome P450

- AFM is unique for probing the interaction between proteins or between protein and membranes, which are all critical for modulating the function of proteins.
- Detection of these interactions are challenging for other microscopy or spectroscopy techniques --- too much interferences.
- AFM provides double functions --- precise positioning (probing) and force measurement.
- One technique requirement --- immobilization of lipid bilayer (*avoid collapse and maintain the biological activity*), on which the cytochrome P450 can be embedded.

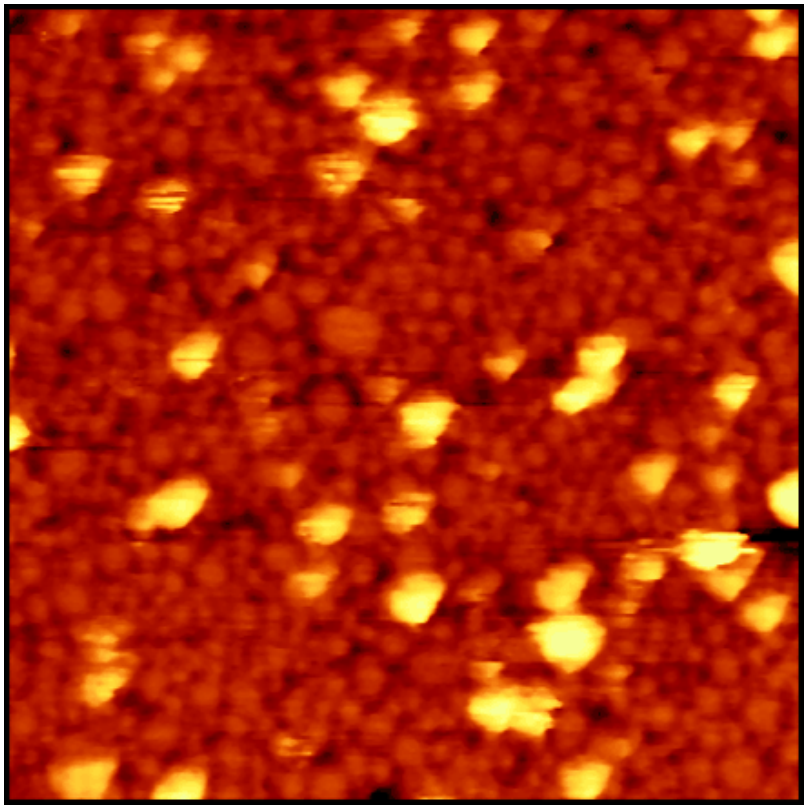

Height image of cytochrome P450 at the rHDL surface on a freshly cleaved mica surface. The image was obtained in contact mode. The image size is 500 × 500 nm.

Sligar,PNAS,2002,99,6725-6730

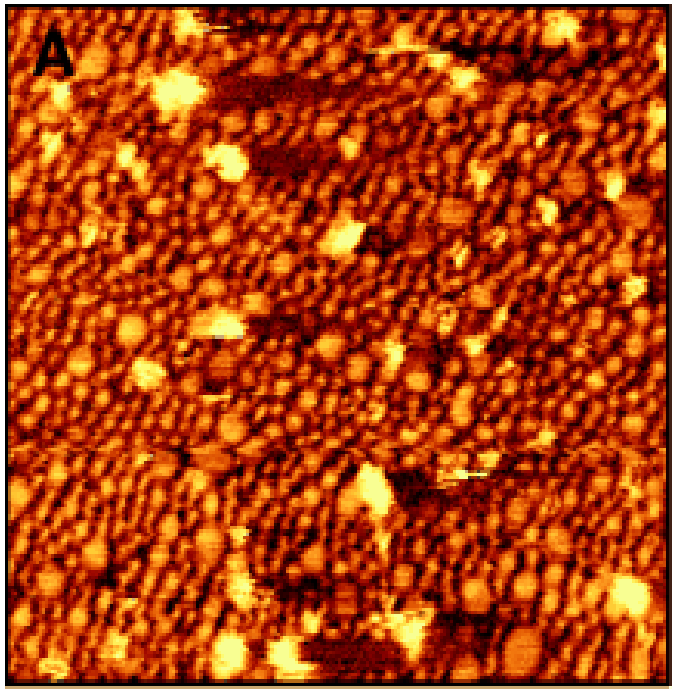

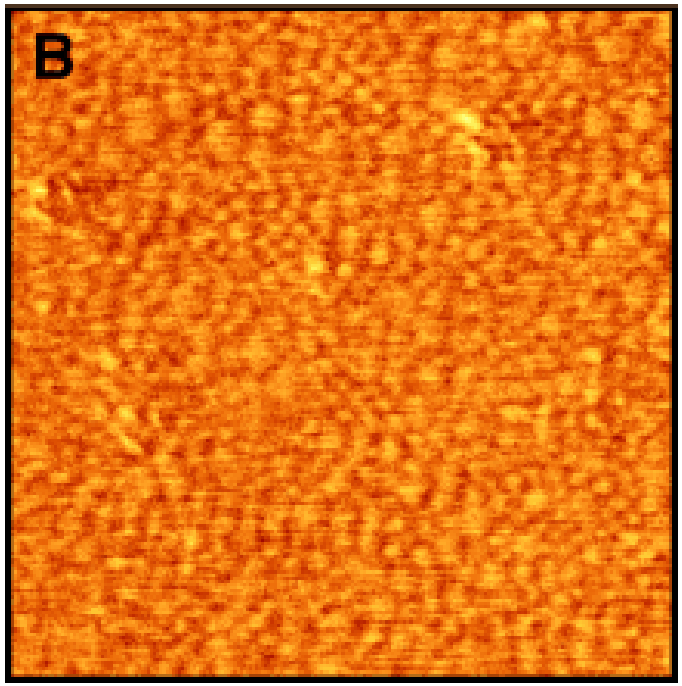

Images of P450

before (*A*)

and after (*B*)

in situ treatment with 15 µg/ml trypsin.

The image in *B* was taken approximately 10 min after addition of trypsin.

Images are contact images in deflection mode. The image size is 500 × 500 nm.

Sligar,PNAS,2002,99,6725-6730

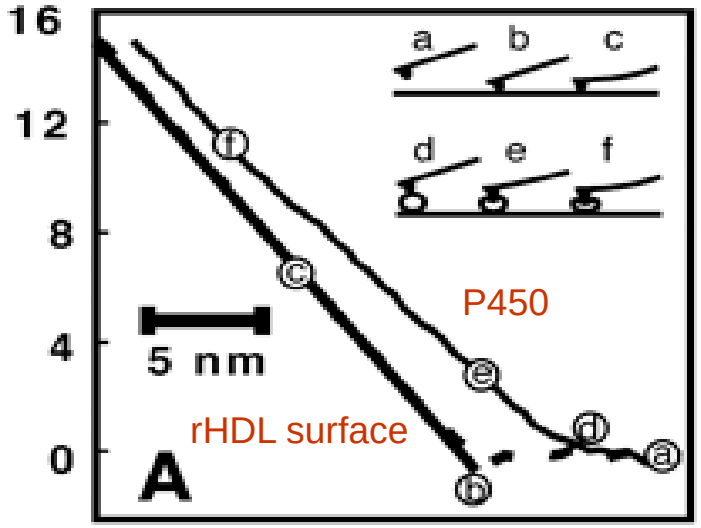

Tip height over the sample

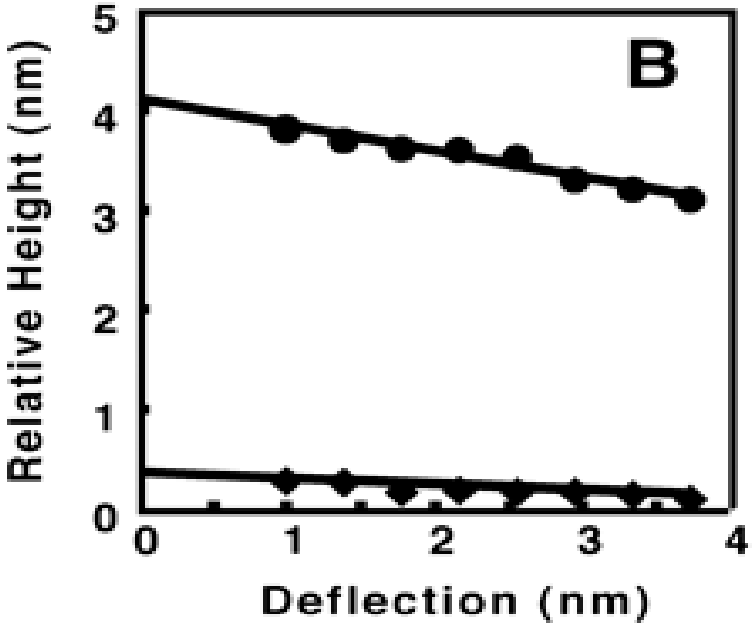

(A) Force curve in approach direction taken on a cytochrome P450 molecule (thin line), rHDL surface (dashed line), and theoretical hard surface (thick line). Curves are averages of several force curves. (*Inset*) Regions of force curves on a hard surface [(*a*) noncontact, (*b*) point of contact, and (*c*) region of constant compliance] and on a protein [(*d*) region of contact with protein, (*e*) deformation, and (*f*) region of constant compliance].

(B) Relative height as a function of cantilever deflection. Lines are least squares fits with intercepts of 0.39 ± 0.03 nm (rHDL) and 4.13 ± 0.06 nm (CYP2B4) giving an extrapolated height for CYP2B4 above the rHDL surface of 3.74 ± 0.07 nm.

Non-linearity is due to other kinds of tip-surface interactions.

Sligar,PNAS,2002,99,6725-6730

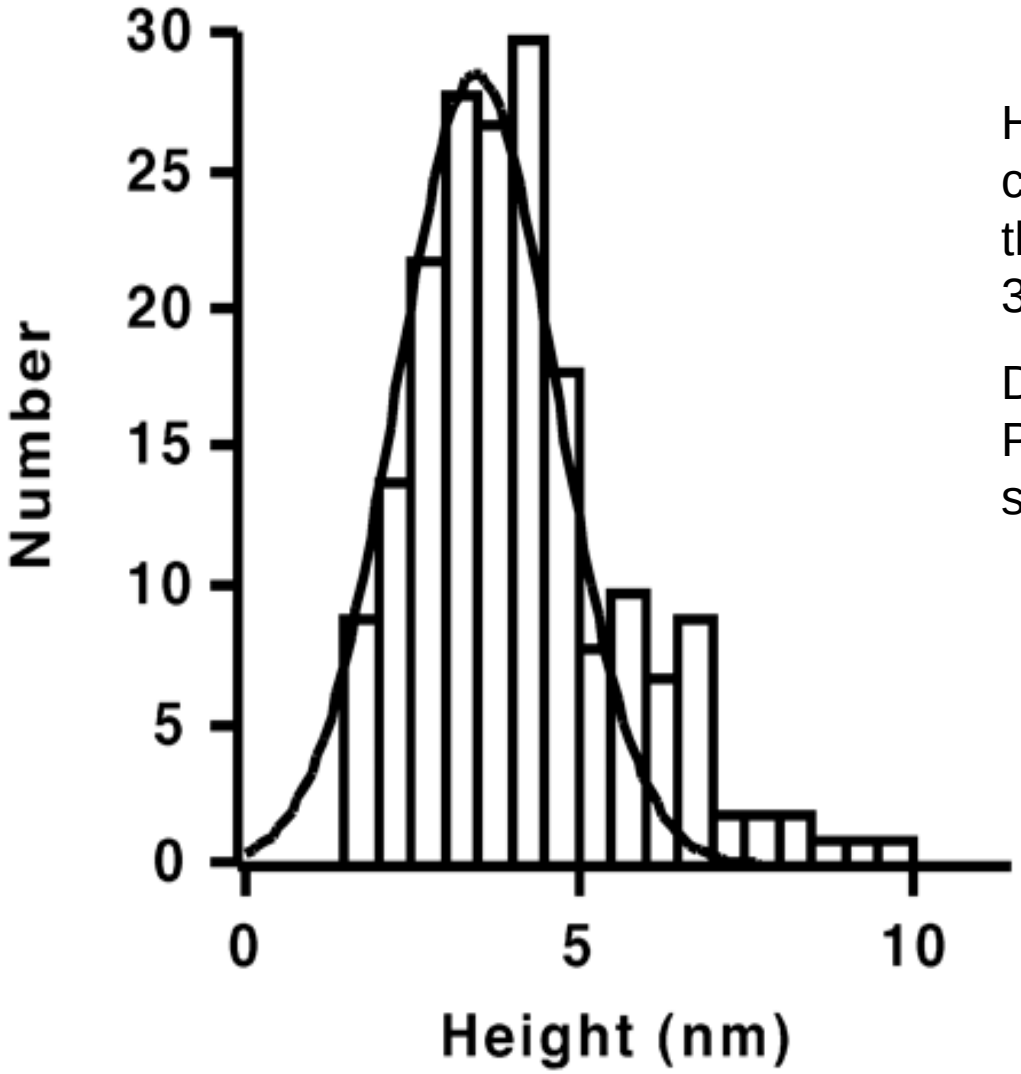

Histogram of the height of cytochrome P450 molecules above the rHDL surface, having a peak at 3.5 nm with a SD of 0.9 nm.

Data were taken for 191 cytochrome P450 molecules from 12 areas of a sample.

Sligar,PNAS,2002,99,6725-6730

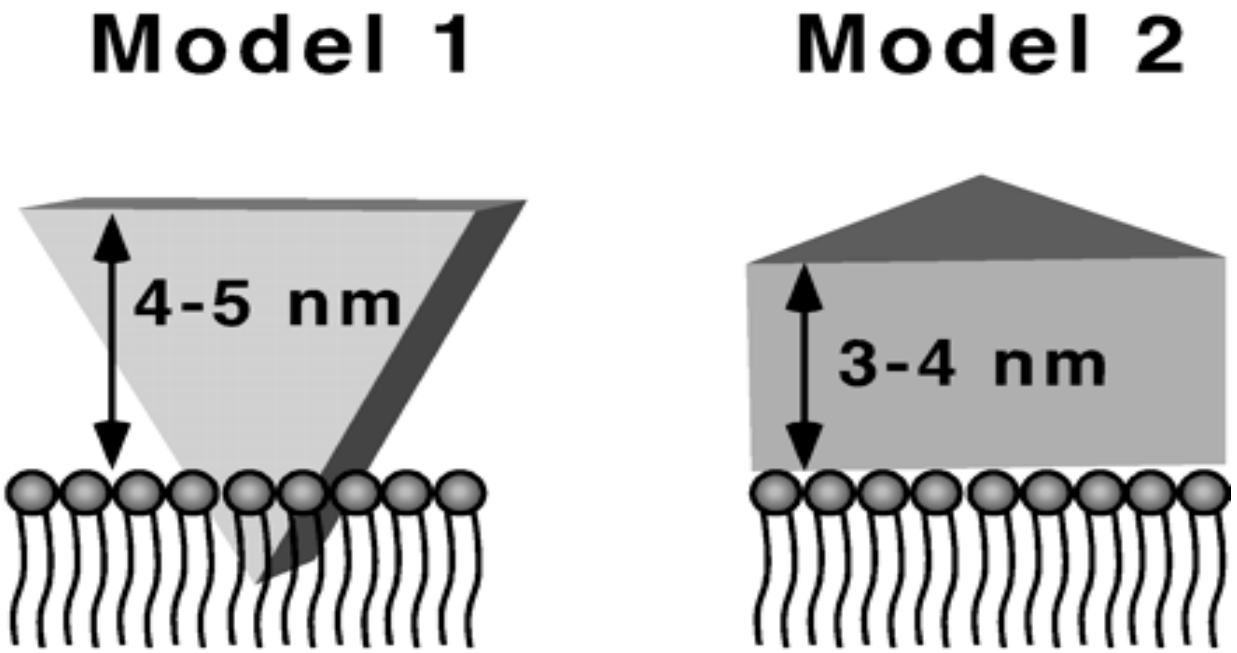

Schematic of P450 interacting with the phospholipid bilayer domain of rHDL.

In Model 1, a hydrophobic tip is inserted into the membrane and the heme is perpendicular to the membrane --- this mode is more likely.

In Model 2, the enzyme is lying on its distal face with the heme parallel to the membrane. The transmembrane anchor domain is not shown.

Sligar,PNAS,2002,99,6725-6730

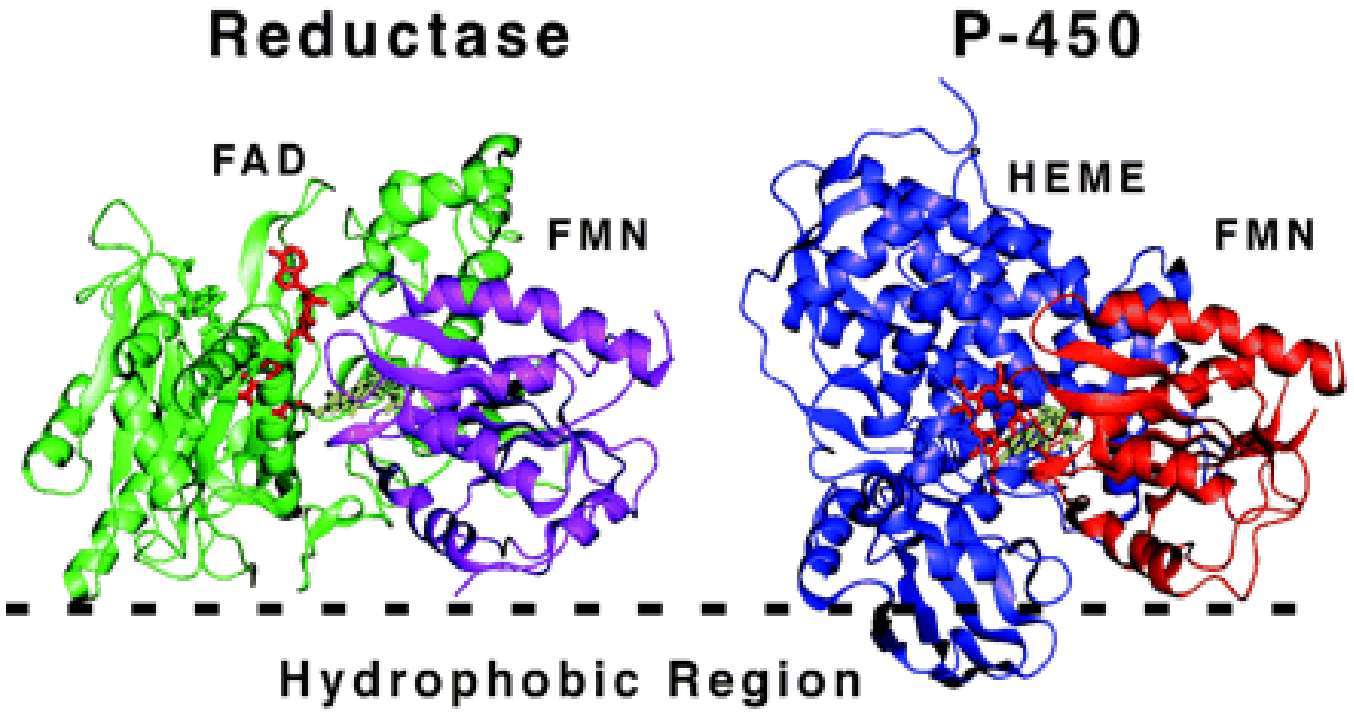

Possible orientation of redox transfer complexes on the membrane surface.

Cytochrome P450 reductase is shown based on the probable orientation of the reductase at a membrane surface (hydrophobic region).

Cytochrome P450 was oriented such that the FMN domain (orange) of the known structure of bacterial cytochrome P450 CYP102 is roughly superimposable on the FMN domain of P450 reductase (purple).

The resulting orientation of cytochrome P450 with respect to the membrane corresponds to Model 1 of last figure. Note that whereas the FMN (yellow) of reductase accepts electrons from FAD (green), in the P450 structure the FMN (yellow) is in close proximity to the heme cofactor (red).

Sligar,PNAS,2002,99,6725-6730

Example # 3: Voltage and pH-induced channel closure of porin OmpF

Daniel J. Müller and Andreas Engel

M. E. Müller-Institute for Microscopy, Biozentrum University of Basel
Klingelbergstrasse 70 CH-4056, Basel, Switzerland

Porin is a ***channel*** protein in *Escherichia coli* outer membrane

Müller,JMB,1999,285,1347

Background

- Gram-negative bacteria are protected by an outer membrane in which trimeric channels, the porins, facilitate the passage of small solutes.
- An *E. coli* outer membrane contains approximately 105 porins to allow the passage of solutes <600 Da.
- The pores are formed by membrane-spanning antiparallel β-strands, which are connected by short turns on the periplasmic side and long loops on the extracellular side.
- Voltage and pH-dependent conformational changes of these extracellular loops have now been visualized by AFM of two-dimensional crystals of *Escherichia coli* porin OmpF.
- Closure of the channel entrance --- a mechanism that the cells have evolved to protect themselves from drastic changes of the environment.

Müller,JMB,1999,285,1347

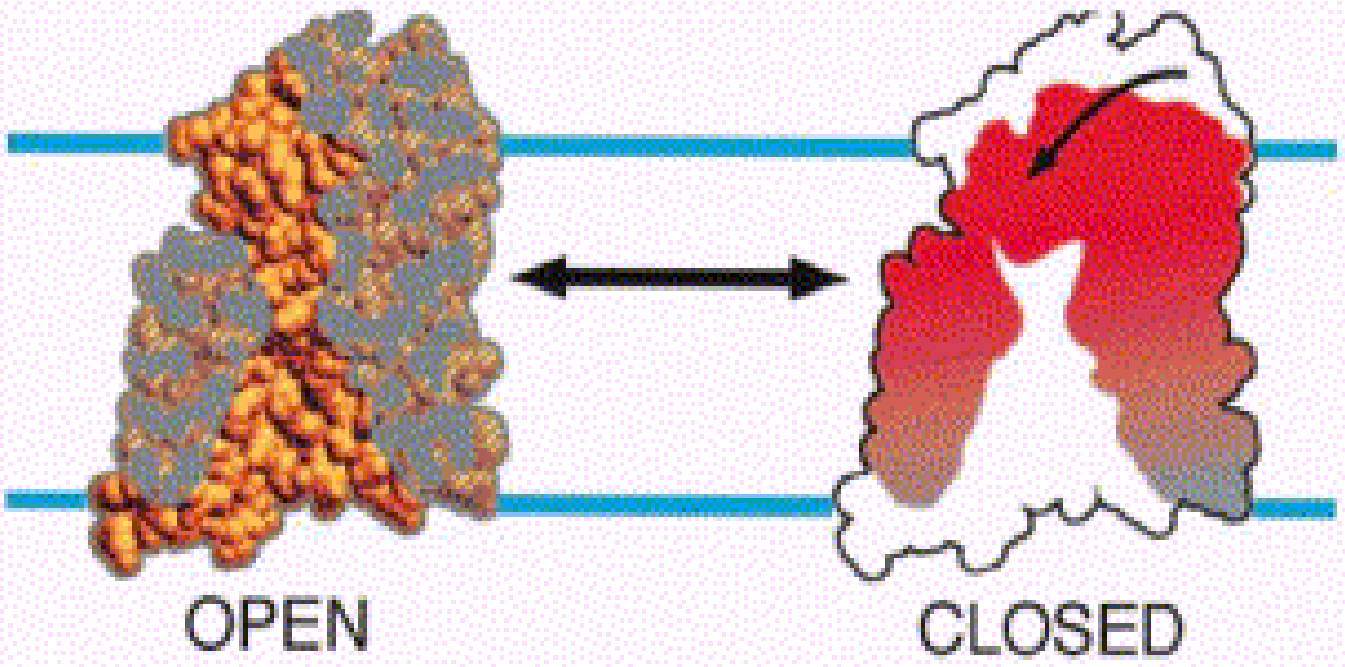

The conformational change of porin OmpF induced by either low pH or a membrane potential can be modeled as a rotation of the extracellular domain about a hinge at the rim of the β -barrel. A cross-section of the monomer demonstrates the open conformation (left porin monomer), and the closed conformation (right monomer). The black arrow indicates the putative rotation of the extracellular domain, while the membrane surface is indicated by blue lines.

Müller,JMB,1999,285,1347

Compared to electronic microscopy imaging that is usually applied to dead biological species and requires metallic stain, AFM enables in situ imaging of living cells and species, through non-damaging imaging mode.

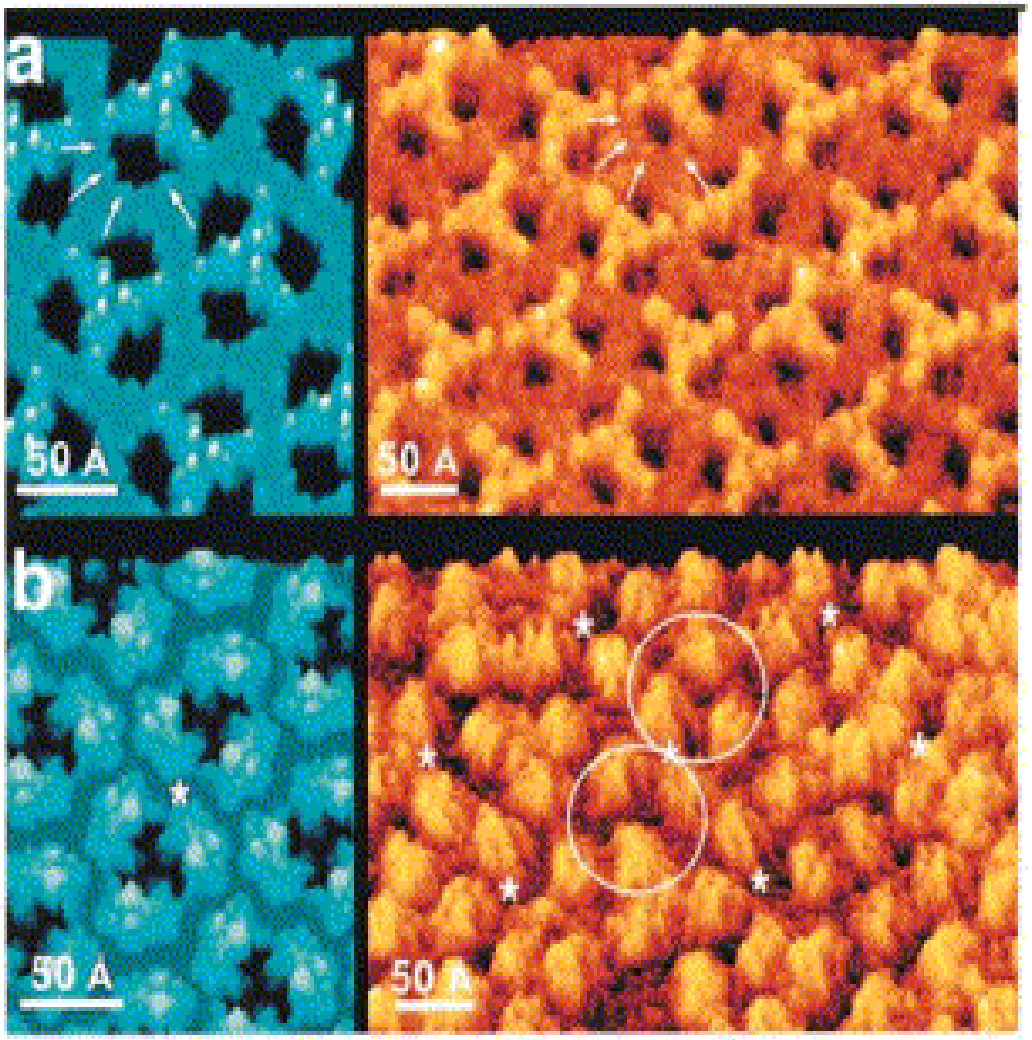

(a) Periplasmic surface; arrows indicate short β-strand-connecting turns that can sometimes be seen in the topographs.

(b) Extracellular surface; domains formed by long loops protrude by 13 Å away from the membrane and are flexible, leading to a disordered appearance.

The 2-fold centers of rectangular unit cells determined by cross-correlation of the topograph with the atomic model are indicated by asterisks, while two porin trimers with their triangular vestibules are marked with circles.

Crystals were adsorbed to mica in 20 mM Tris-HCl (pH 7.8), 0.3 M KCl and incubated for 30 minutes.

Müller,JMB,1999,285,1347

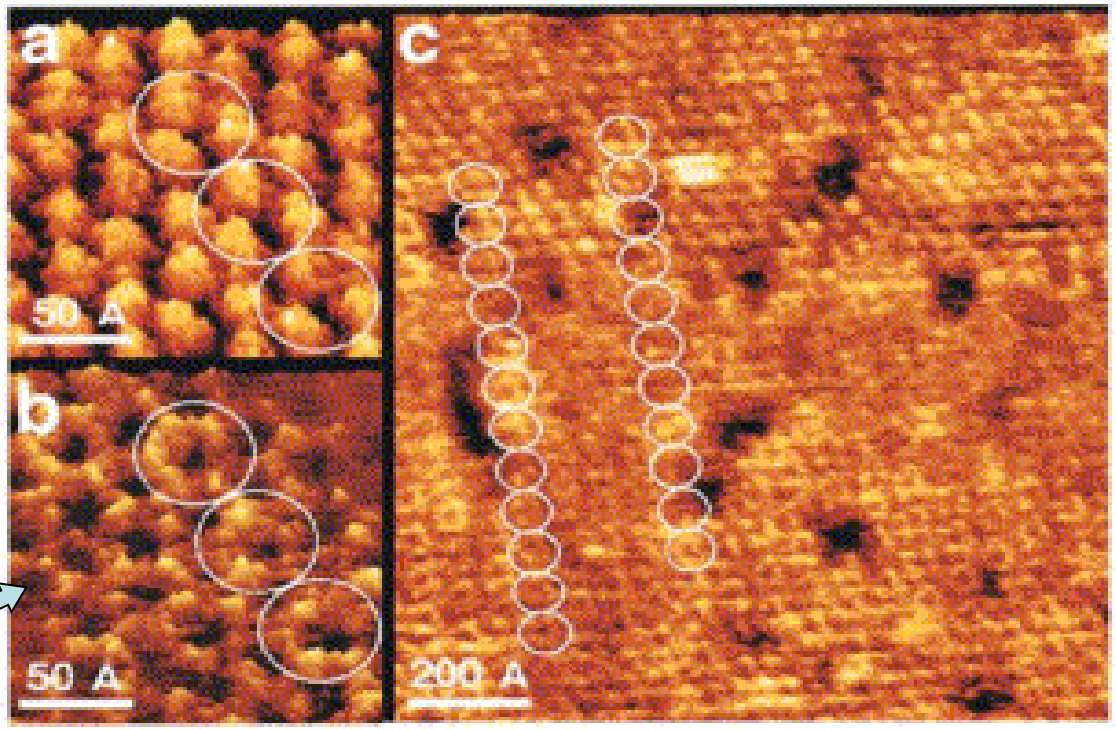

Crystals were adsorbed to HOPG and topographs taken in 10 mM Tris-HCl (pH 7.8), 50 mM KCl.

Voltage-induced conformational change of the extracellular surface of porin OmpF.

(a) Trigonally packed porin trimers (marked by ellipses) exhibit 13 Å long protrusions surrounding a triangular vestibule.

(b) Upon application of a membrane potential, a dramatic conformational change occurs: the extracellular domains convert into doughnuts of about 6 Å height, marked by circles.

(c) Sometimes both conformations were observed simultaneously, allowing the center of the trimer in its extended conformation to be correlated with the center of the doughnuts, as indicated by rows of circles.

Müller,JMB,1999,285,1347

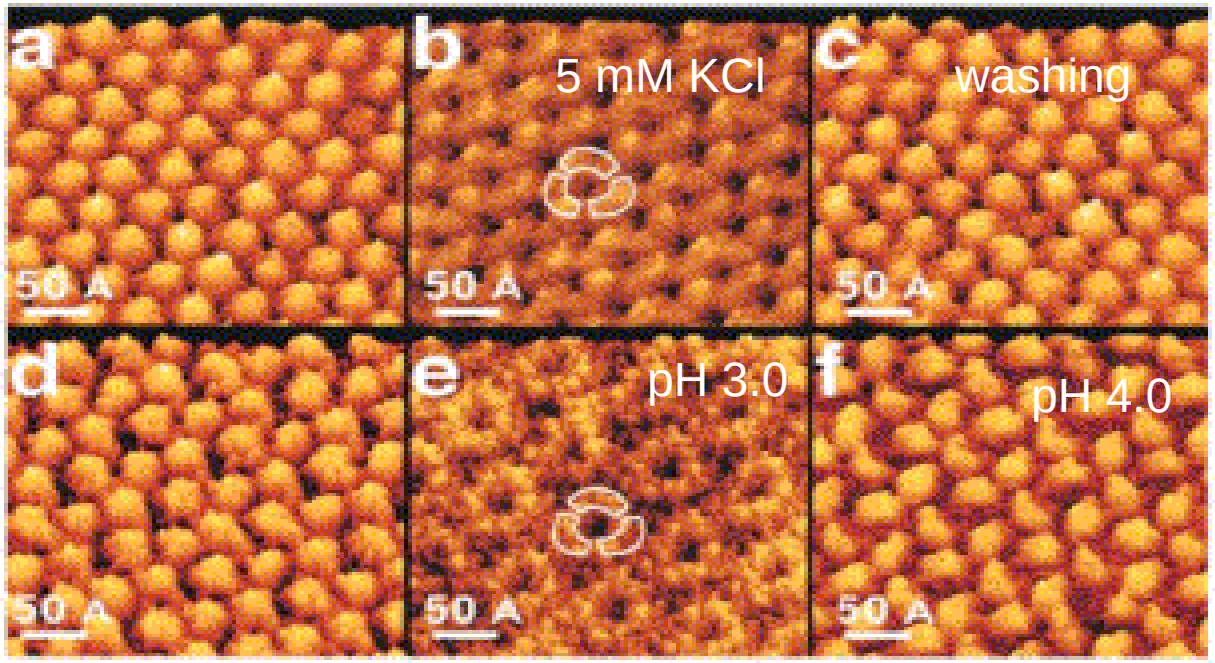

Ion gradient and **pH-dependent** conformation of porin OmpF (on mica).

(a) The extracellular surface of a trimer porin membrane.

(b) After exposure to 5 mM KCl (5 mM Tris-HCl, pH 7.8), a low ionic buffer, extracellular domains collapsed into doughnut-like structures of 6 Å height.

(c) Topograph of the same area observed after flushing the liquid cell with the high-ionic-strength buffer had fully extended extracellular protrusions.

(d) Porin trimers with domains showing a small indentation at the top and a distinct vestibule about the 3-fold axis were imaged at pH 7 (20 mM Tris, 0.3 M KCl), a little lower pH.

(e) An area of the same crystal recorded at pH 3 (20 mM citric acid, 0.3 M KCl) exhibited doughnut-like structures of 6 Å height.

(f) Upon increasing the pH to 4, the protrusions had a height of 12 Å.

Müller,JMB,1999,285,1347

NATURE|Vol 440|2 March 2006

FOCUS ON THE LIVING

Atomic force microscopes have revolutionized the study of materials, but probing watery biological systems has proved more difficult. **Jenny Hogan** asks whether a fix is at hand.

Bart Hoogenboom's windowless room is a cramped space, almost filled by the sturdy table at its centre. Cables dangle from piles of electrical devices that climb to the ceiling. In the midst of the tangle of equipment is a stack of three small metal cylinders. Hidden inside the top one is a sliver of silicon, its tip quivering up and down 200,000 times each second.

"It is an experimental physicist's dream and a biologist's nightmare," says Hoogenboom. Happily, Hoogenboom is a physicist, a postdoc at the University of Basel in Switzerland, and for him the roomful of gadgetry to tinker with is a treat. But the outcome of his tinkering could enrich the lives of biologists

The cylinders on the table are the working parts of an atomic force microscope, or AFM. Invented 20

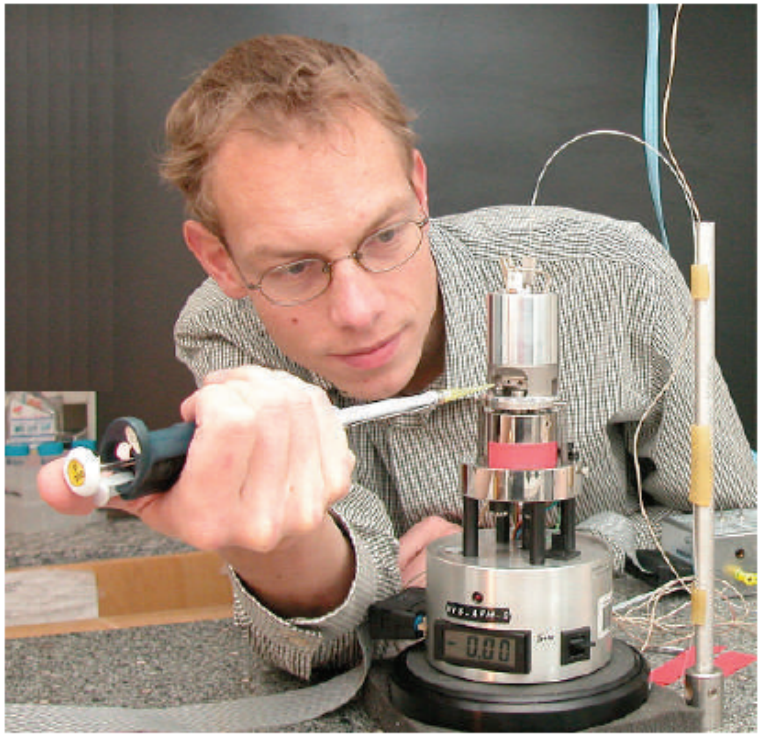

Physicist Bart Hoogenboom's love of gadgetry could pay off for biologists.

P. REIMANN

the tip and moved back and forth and from side to side. But it is not the most precise way of doing things. The AFM tip tends to damage or dislodge the things it is scanning, which degrades the image resolution and limits the types of sample the technique can be used to study.

The obvious solution is to make the tip behave more gently when scanning the samples, and it is to this end that various researchers have turned to the 'frequency modulation' or FM mode. In FM mode, the tip hovers just above the surface under study. A pulse of energy is used to make the cantilever tremble, and the topography of the surface below affects the frequency at which it does so. So long as the forces that the tip senses as it hovers above the surface can be inferred from changes to the cantilever's frequency, the tip doesn't actually have

way the cantilever's deflection was being measured. He thought this might compensate for the water damping down the oscillations.

In most commercial AFMs, a laser beam is bounced off the top surface of the cantilever to work out the tip's position. Fukuma and his co-workers set to improving each element of this sensor system, boosting the laser power and introducing a technique used in CD-ROM and DVD drives to stabilize the laser performance. The combined effect of the changes was to reduce the noise in the system to near its theoretical limit[3]. Without even trying to minimize the noise from other sources, such as the buffeting of the cantilever by water, the team got striking results. "I did just a few experiments to get atomic resolution," says Fukuma. In July last year, the research team reported their findings[4]. The paper's centrepiece is an image of mica taken in pure water, showing the atoms which are just half a nanometre wide.

Scaling down

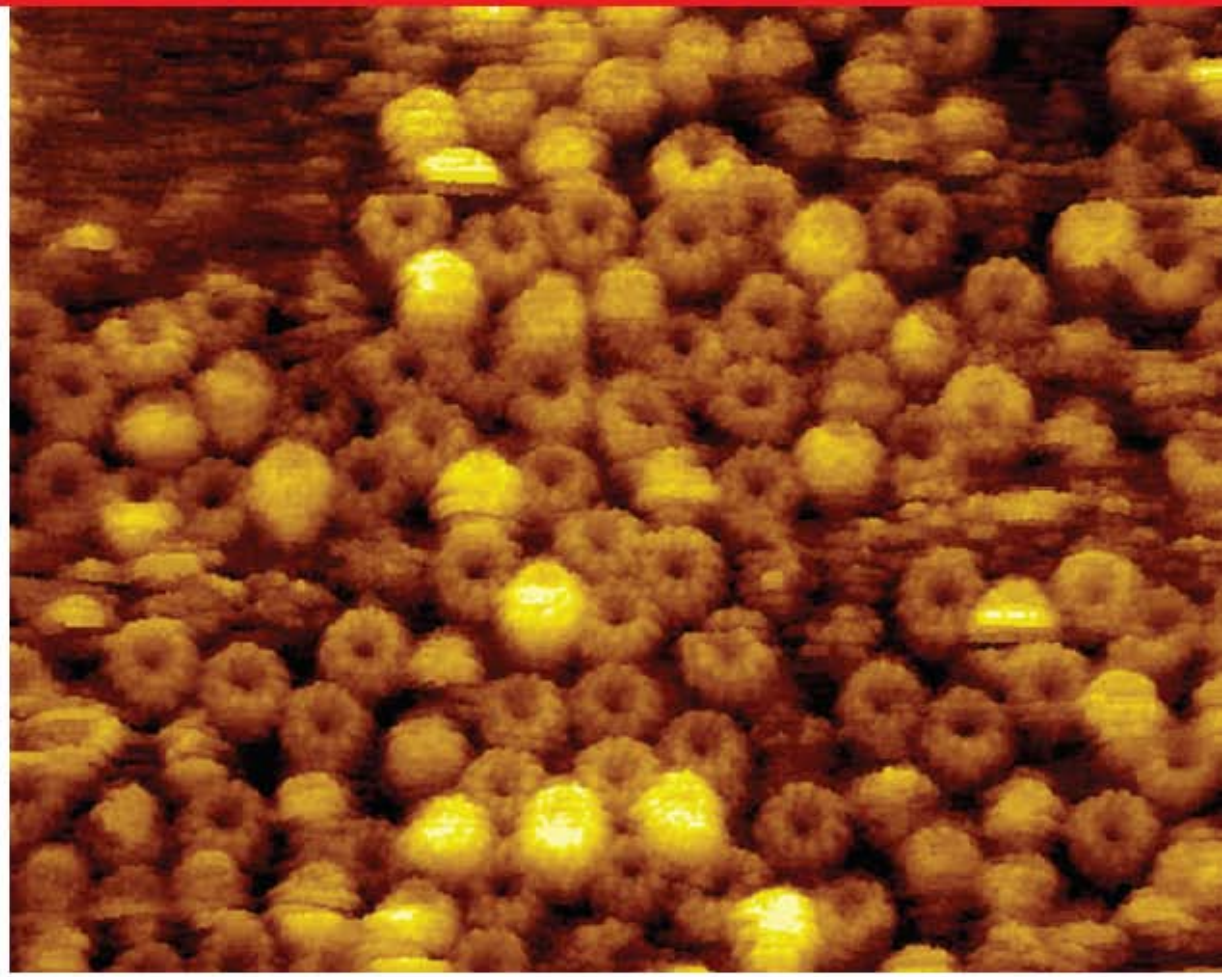

Atomic force microscopy has revealed the detailed structure of energy-converting ATPase rotor rings[6].

Example # 4: Amyloid-β (Aβ) peptides vs. Alzheimer disease

Aβ fibers

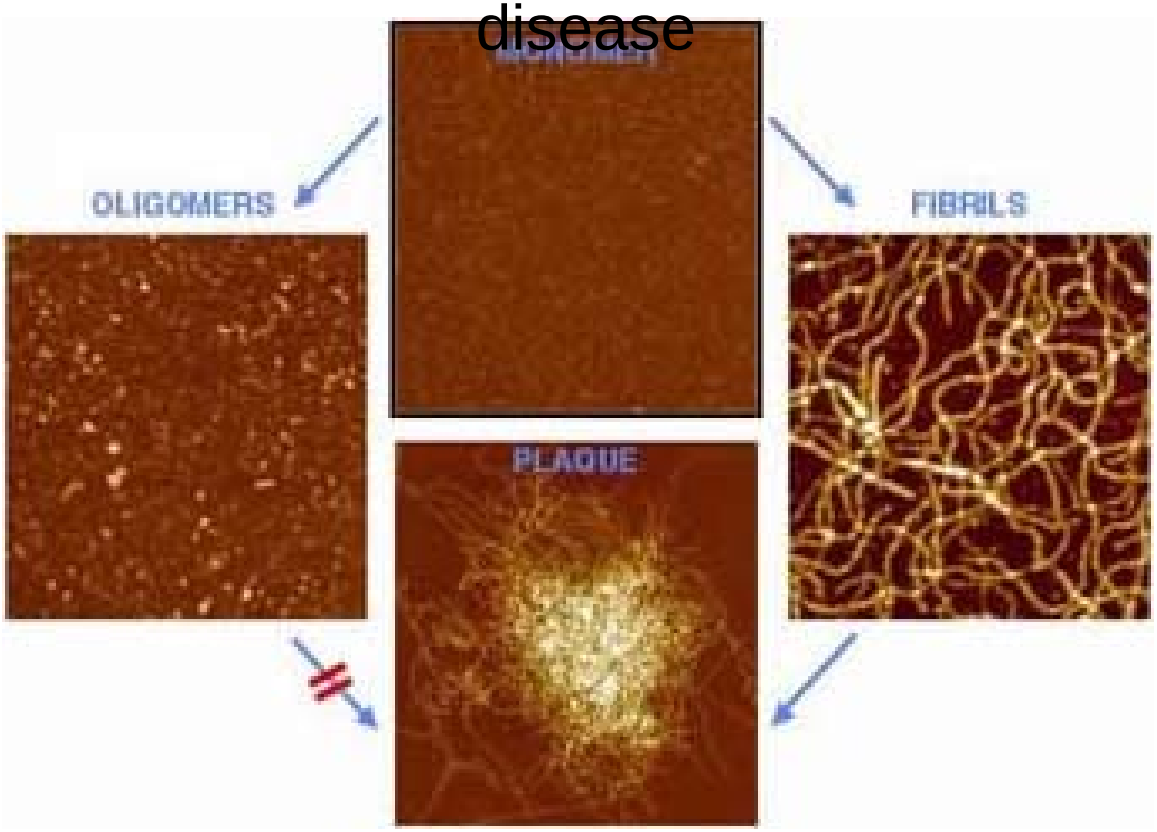

Alzheimer's patient brain: *the generalized cerebral cortical atrophy*. *(Courtesy of JE Parisi, Mayo Clinic, Rochester, Minnesota.)*

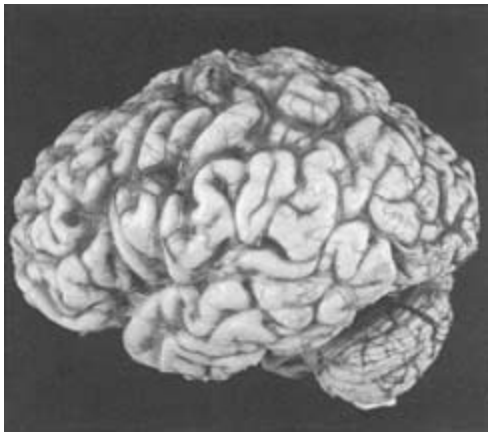

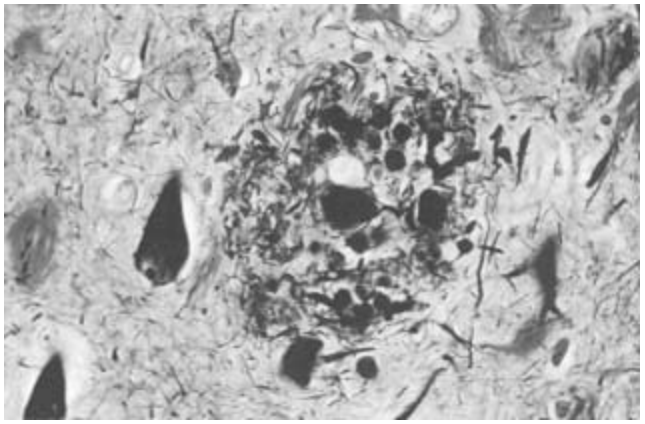

Photomicrograph of entorhinal cortex in Alzheimer's disease. The neuritic plaque is composed of an amyloid core surrounded by dystrophic neurites. The dark flame-shaped fibrillar structures are neurofibrillary tangles.

Example # 4: Amyloid-β (Aβ) vs. Alzheimer disease

- Alzheimer disease (AD) is the most prevalent form of late-life mental failure in humans. In the AD patient brain, striking ultrastructural changes include: neuritic plaques and neurofibrillary tanglesm, which both consist of Aβ.
- Over the age of 70, > 10% of people experience memory loss;

  Over the age of 85, 25-50% of people experience memory loss;

  Over the age of 90, ~90% of people experience memory loss.
- Aβ is derived from a large protein, amyloid precursor protein (APP), by sequential proteolytic cleavages, which involve three proteases, α-secretase, β-secretase and γ-secretase.
- Aβ42 has the highest propensity for aggregation and fibrillogenesis.

Alzheimer's Disease

Treatment and Prevention

Strategy 1: β and γ secretase inhibitor

Strategy 2: Aβ aggregation inhibitors

Strategy 3: lowering cholesterol levels

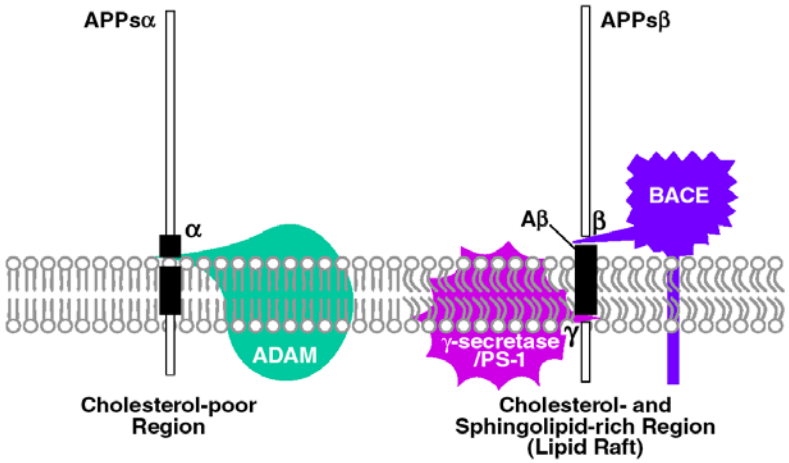

Nontoxic fragments

Aβ peptide

apoE4

Zn^{++}/Cu^{++}

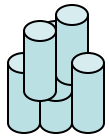

+ apoE

Aggregates/fibrils

Challenges for traditional microscopies and spectroscopies in detecting Aβ

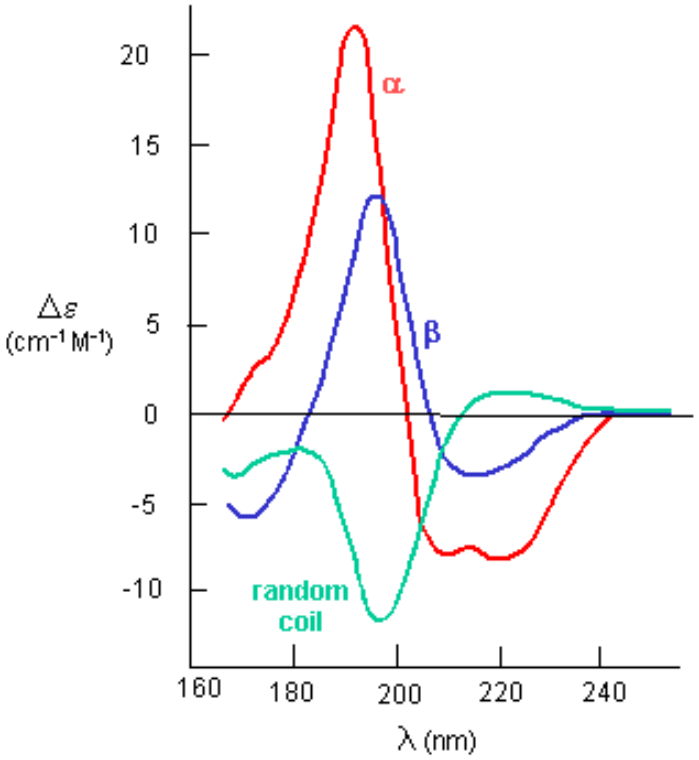

- TEM: suffering from the fragile structure of Aβ aggregates.
- SEM: suffering from non-conductivity and the low resolution.
- CD (circular dichroism): low sensitivity to detect small amount of short fibrils, which might act seeds for the growth of larger fibrils. *See the slide for CD characterization of α-helix, β-sheet and random coil of peptide chains.*
- **AFM can detect trace amount of fibrils by scanning multiple areas and performing statistics -- sensitivity < 0.1%.**

In Vitro Characterization of Conditions for Amyloid- Peptide Oligomerization and Fibrillogenesis

W. Blaine Stine Jr. , Karie N. Dahlgren , Grant A. Krafft, and Mary Jo LaDu

Department of Medicine, Division of Geriatrics, Evanston Northwestern Healthcare Research Institute, Evanston, Illinois 60201;

Departments of Molecular Pharmacology and Neurobiology and Physiology and Alzheimer's Disease Core Center, Northwestern University, Chicago, Illinois 60611.

LaDu, *J. Biol. Chem*., 2003, 278, 11612

Experimental design and improvement

- Challenge: *make sure the starting materials (peptides) are purely in monomeric state* --- HFIP proved the best for solubilizing monomeric Aβ.
- Here is the first study using a single chemically and structurally homogeneous unaggregated starting material to investigate formation of fibrils depending on various solution parameters.
- It was found --- the formation of oligomers, fibrils, and fibrillar aggregates is determined by time, concentration, temperature, pH, ionic strength, and Aβ species.

- AFM measurement was carried out on dry surface of mica (atomic smooth).
- Sample preparation: deposit → rinsing with water (*peptide stays while salts washed away*) → dried in air.

LaDu, *J. Biol. Chem*., 2003, 278, 11612

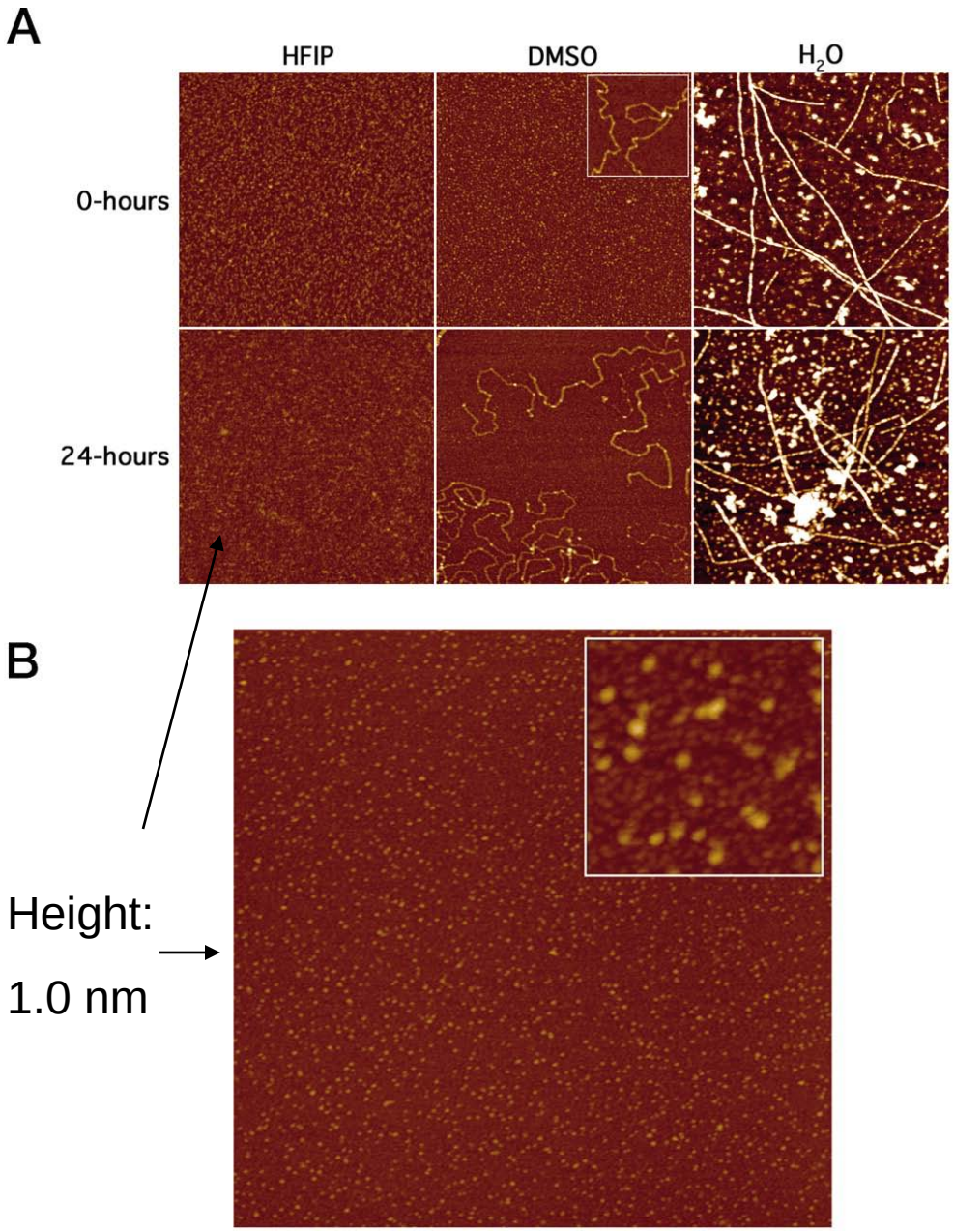

AFM analysis of A 1-42 solubilized in HFIP, DMSO, and H2O.

A, lyophilized synthetic A 1-42 was solubilized to 5 mM in 100% HFIP, DMSO, or deionized H2O. 5 mM stock solutions were incubated for 24 h at room temperature. Samples before (*0-h*) and after incubation (*24-h*) were mounted for AFM analysis at 10 µM. Representative 1 × 1-µm x-y, 5-nm total z-range AFM images are shown. *Inset image*, 390 × 390 nm x-y, 5-nm total z-range.

B, HFIP-treated lyophilized peptide stocks were resuspended to 5 mM in DMSO and diluted to 10 µM for AFM analysis. Representative 2 × 2-µm x-y, 5-nm total z-range AFM image is shown. *Inset image*, 200 × 200-nm x-y, 5-nm total z-range.

LaDu, *J. Biol. Chem*., 2003, 278, 11612

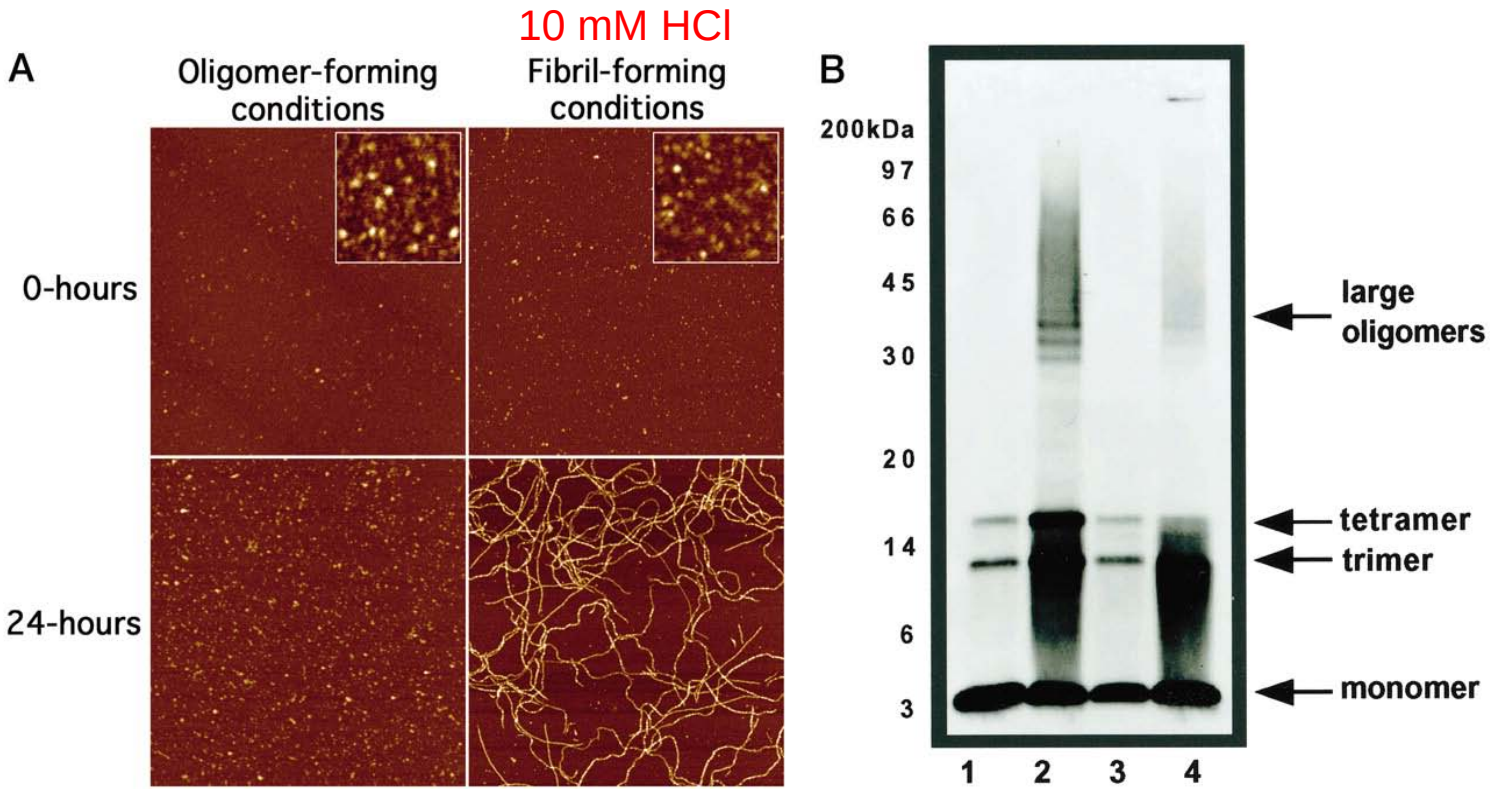

Solution conditions for the formation of oligomeric or fibrillar Aβ 1-42 assemblies.

A, AFM. 5 mM HFIP-treated Aβ 1-42 in DMSO was diluted to 100 µM in ice-cold F-12 culture medium for oligomers and 10 mM HCl for fibrils. Oligomer and fibril preparations were incubated for 24 h at 4 and 37 °C, respectively. Samples before (*0-h*) and after incubation (*24-h*) were mounted for AFM analysis at 10 µM. Representative 2 × 2-µm x-y, 10-nm total z-range AFM images are shown. *Inset images*, 200 × 200-nm x-y, 2-nm total z-range.

B, Western analysis of SDS-PAGE. The representative figure shows 0- and 24-h oligomers (*lanes 1* and *2*) and fibrils (*lanes 3* and *4*).

LaDu, *J. Biol. Chem.*, 2003, 278, 11612

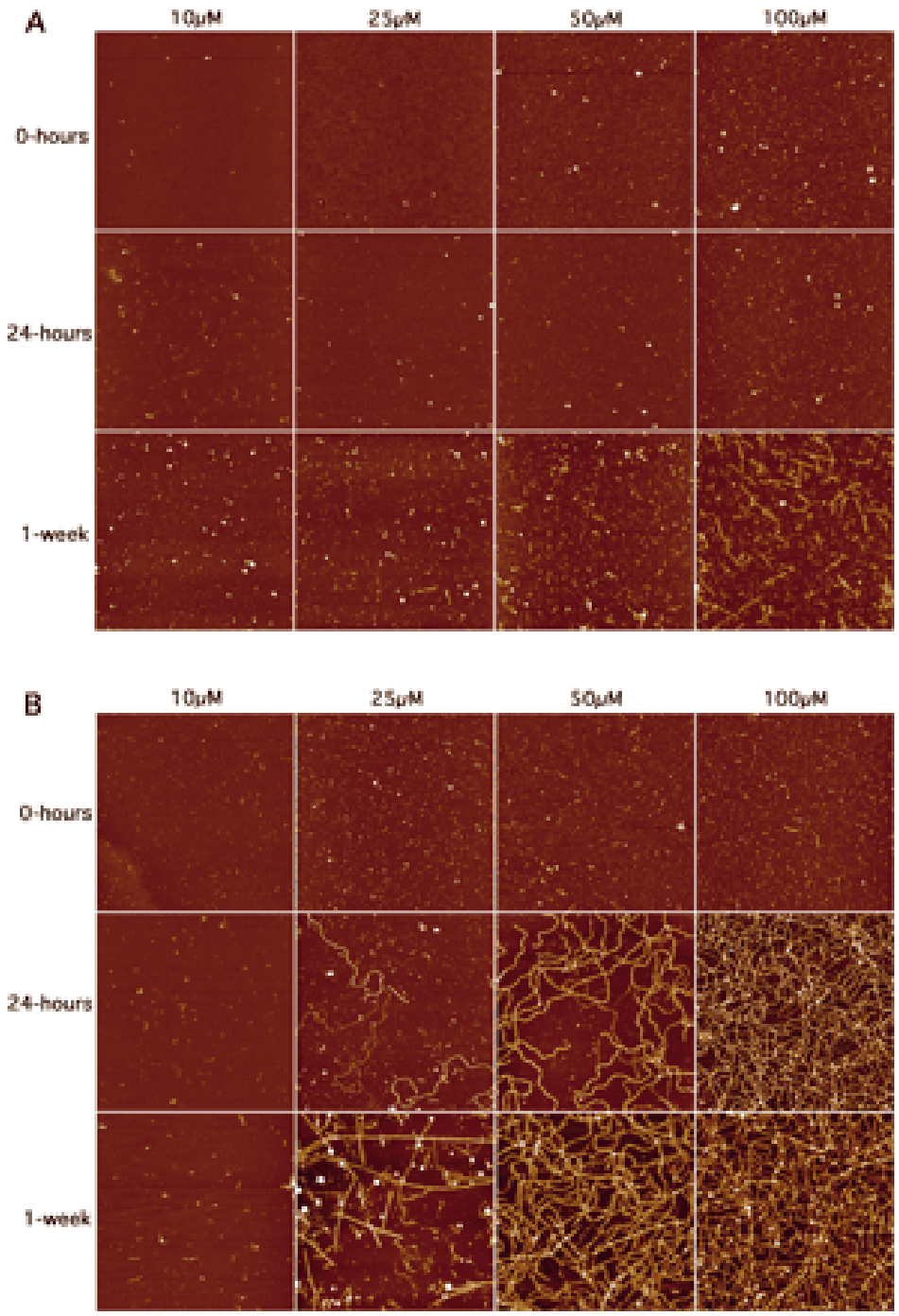

Aβ 1-42 assembly is dependent on incubation time and peptide concentration.

5 mM A 1-42 DMSO stocks were diluted to 10, 25, 50, or 100 μM under

oligomer-forming conditions (*A*) or

fibril-forming conditions (10 mM HCl), (*B*).

Samples were prepared for AFM analysis immediately after dilution (*0-h*), after 24 h, and after 1 week of incubation.

Representative 2 × 2-μm x-y, 10-nm total z-range AFM images are shown.

LaDu, *J. Biol. Chem.*, 2003, 278, 11612

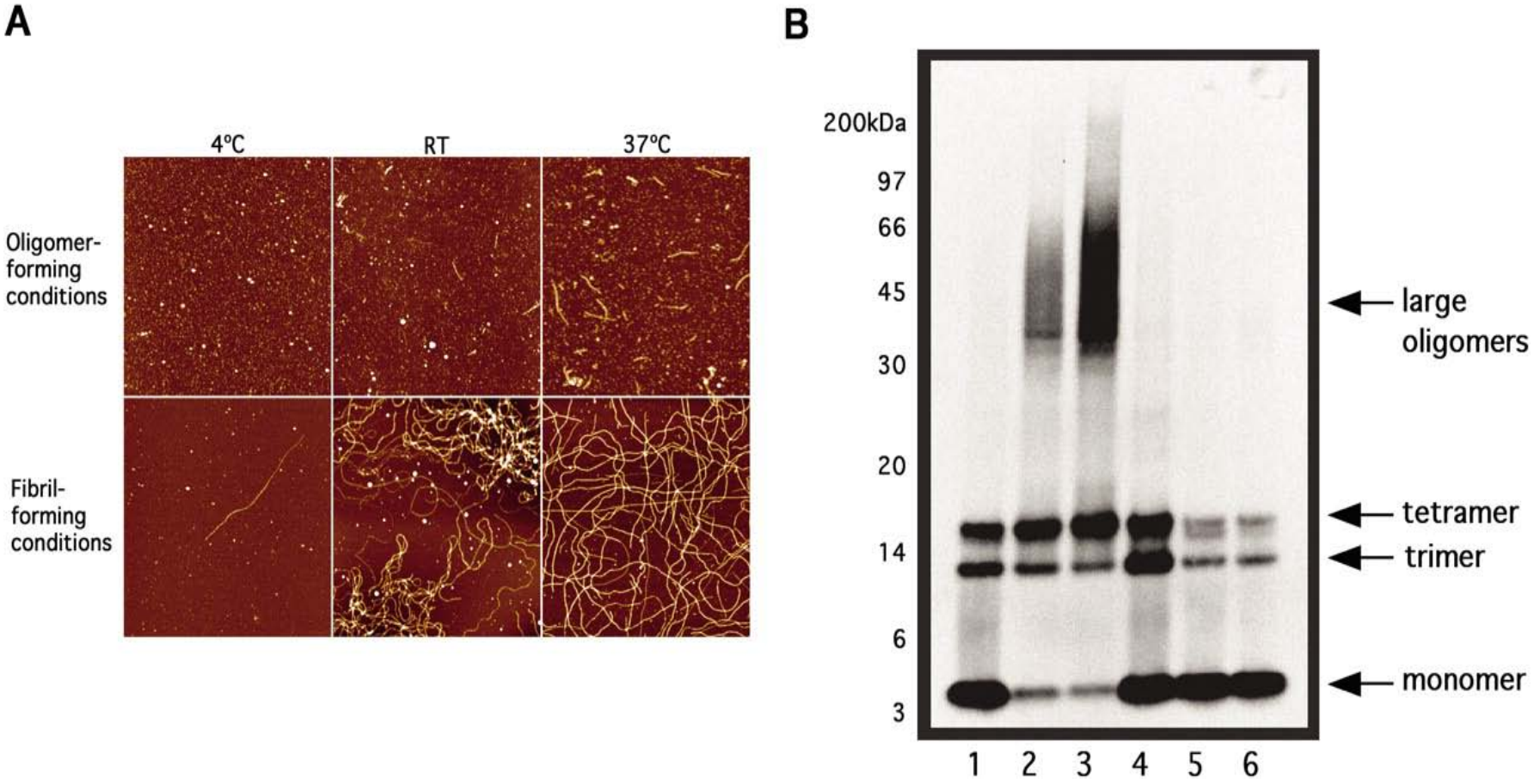

Aβ 1-42 assembly is dependent on temperature.

Aβ 1-42 oligomers and fibrils were incubated at 4 °C, room temperature, or 37 °C for 24 h. Representative 2 × 2-μm x-y, 10-nm total z-range AFM images are shown.

B, Western analysis of SDS-PAGE: oligomers and fibrils at 4 °C (*lanes 1* and *4*), room temperature (*lanes 2* and *5*), and 37 °C (*lanes 3* and *6*), respectively.

LaDu, *J. Biol. Chem.*, 2003, 278, 11612

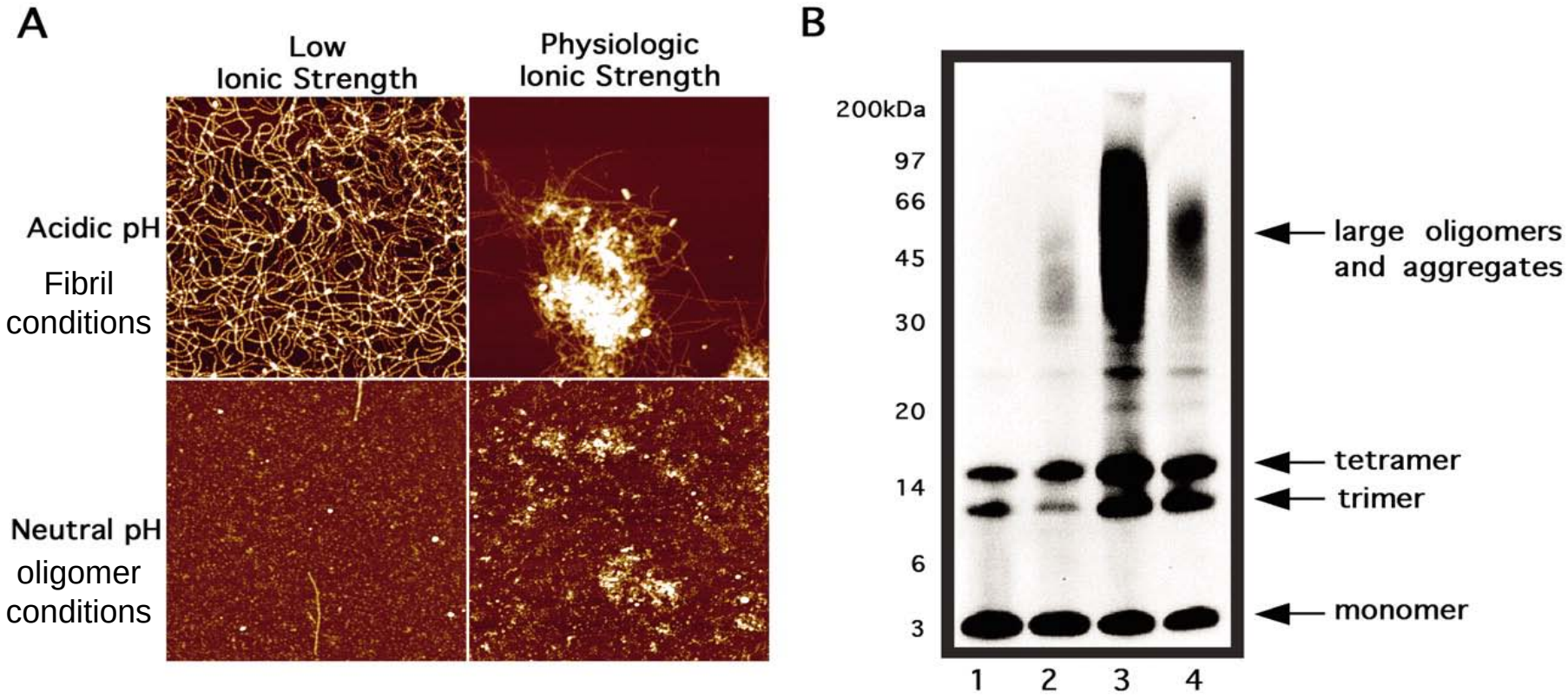

A 1-42 assembly is dependent on ionic strength and pH.

A, 5 mM Aβ 1-42 in DMSO stocks were diluted to 100 µM in either 10 mM HCl (low ionic strength, acidic pH), 10 mM HCl + 150 mM NaCl (acidic pH, physiologic ionic strength), 10 mM Tris, pH 7.4 (neutral pH), or 10 mM Tris, pH 7.4, + 150 mM NaCl (neutral pH, physiologic ionic strength). Samples were prepared after a 24-h incubation at 37 °C.

B, Western analysis of SDS-PAGE: HCl (lane 1), HCl + NaCl (lane 2), Tris (lane 3), and Tris + NaCl (lane 4).

LaDu, *J. Biol. Chem.*, 2003, 278, 11612

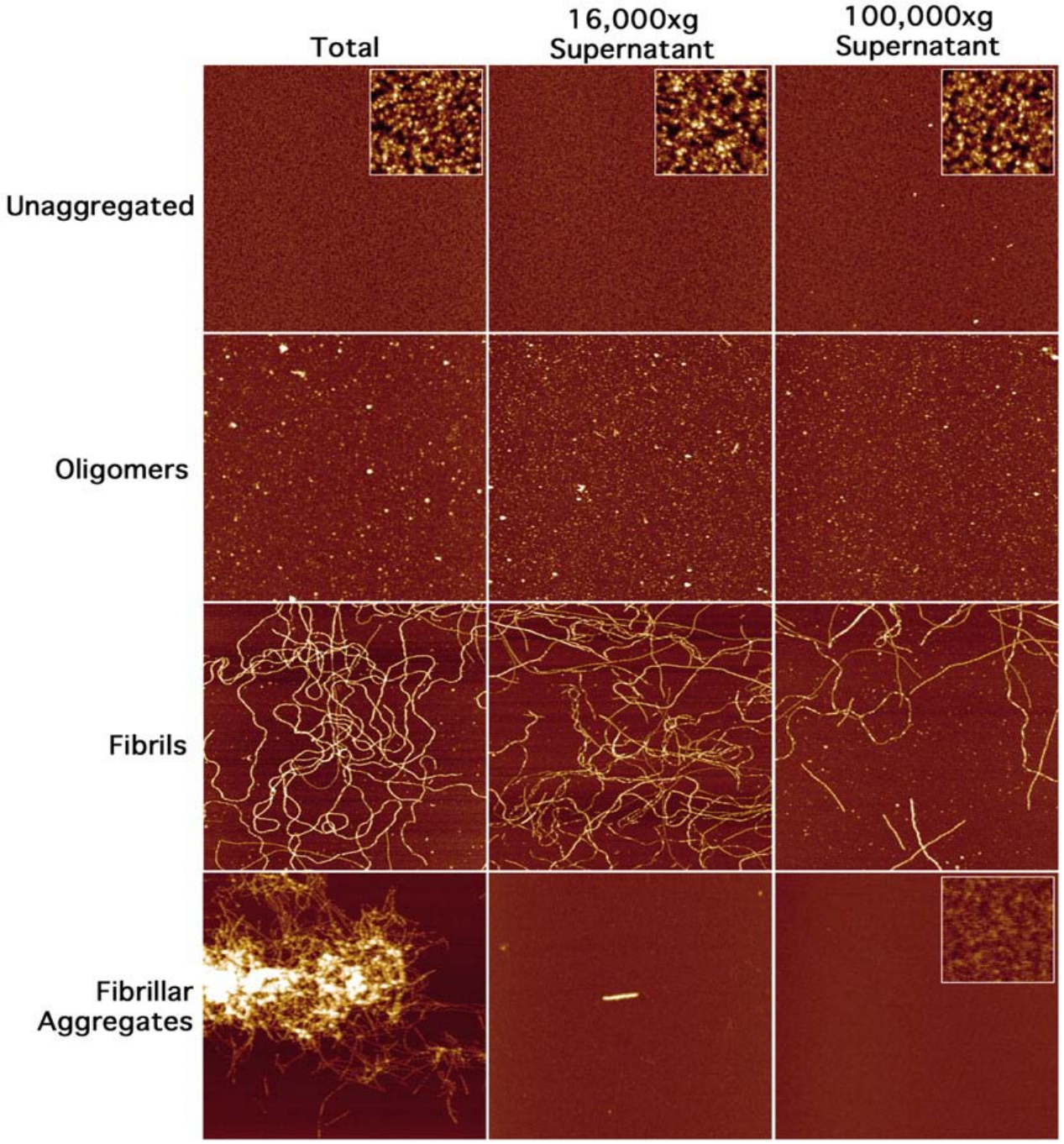

AFM analysis of the solubility of A 1-42 assemblies.

1. Unaggregated solutions of Aβ 1-42 were prepared by dilution of 5 mM A 1-42 DMSO stock solution to 10 μM in ice-cold H2O.
2. Fibrillar aggregates of Aβ 1-42 were prepared by incubation in 10 mM HCl + 150 mM NaCl for 24 h at 37 °C.

LaDu, *J. Biol. Chem.*, 2003, 278, 11612

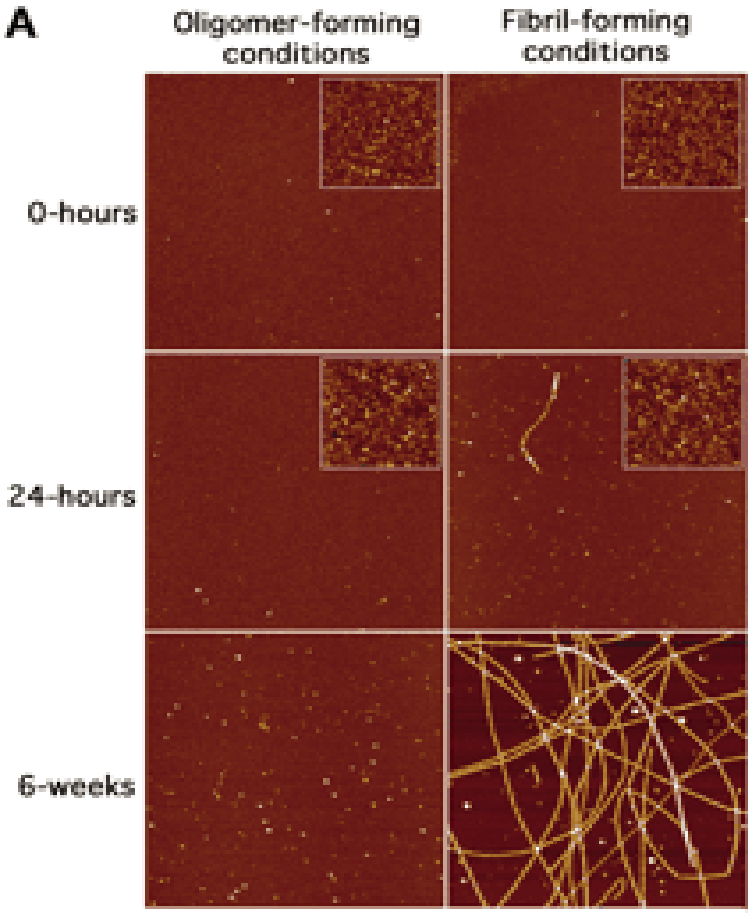

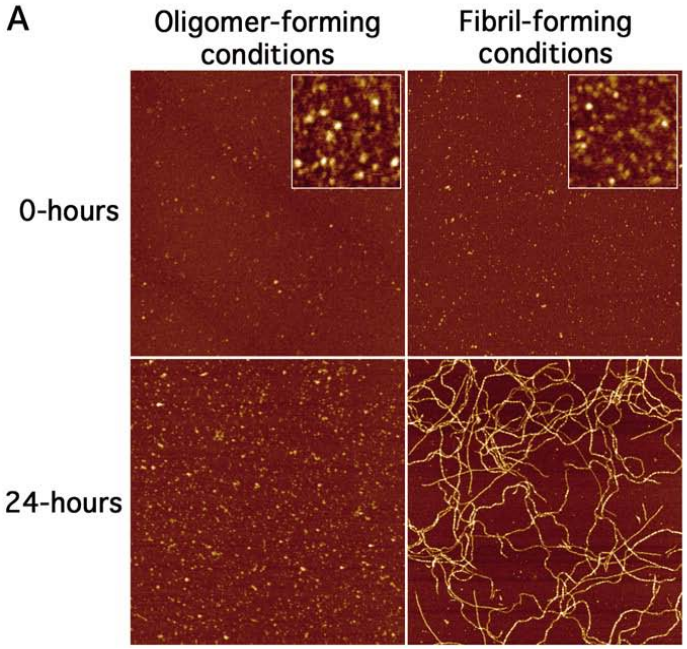

Aβ 1-42

Aβ 1-40 requires longer incubation times to form oligomers and fibrils comparable with Aβ 1-42 oligomers and fibrils.

A, AFM of oligomeric and fibrillar Aβ 1-40 and 1-42 samples were prepared following the same protocol.

B, Western analysis of SDS-PAGE: Oligomers and fibrils were sampled at 0 h (*lanes 1* and *3*), 24 h (*lanes 2* and *4*), and 6 weeks (*lanes 5* and *6*), respectively.

1 2 3 4 5 6